AD

USAAVLABS TECHNICAL REPORT 66-36

FLIGHT TEST EVALUATION OF A DISTRIBUTED SUCTION HIGH-LIFT BOUNDARY LAYER CONTROL SYSTEM ON A MODIFIED L-19 LIAISON AIRCRAFT

By

Sean C. Roberts
Michael R. Smith
David G. Clark

June 1966

U. S. ARMY AVIATION MATERIEL LABORATORIES
FORT EUSTIS, VIRGINIA

CONTRACT DA 44-177-AMC-265(T)
MISSISSIPPI STATE UNIVERSITY
STATE COLLEGE, MISSISSIPPI

Disclaimers

The findings in this report are not to be construed as an official Department of the Army position unless so designated by other authorized documents.

When Government drawings, specifications, or other data are used for any purpose other than in connection with a definitely related Government procurement operation, the United States Government thereby incurs no responsibility nor any obligation whatsoever; and the fact that the Government may have formulated, furnished, or in any way supplied the said drawings, specifications, or other data is not to be regarded by implication or otherwise as in any manner licensing the holder or any other person or corporation, or conveying any rights or permission, to manufacture, use, or sell any patented invention that may in any way be related thereto.

Trade names cited in this report do not constitute an official endorsement or approval of the use of such commercial hardware or software.

Disposition Instructions

Destroy this report when no longer needed. Do not return it to the originator.

DEPARTMENT OF THE ARMY
U. S. ARMY AVIATION MATERIEL LABORATORIES
FORT EUSTIS, VIRGINIA 23604

This report has been reviewed by the U. S. Army Aviation Materiel Laboratories, and is considered to be technically sound.

The work reported is the culmination of research begun by the Aerophysics Department of Mississippi State University (MSU) in the early 1950's involving the phenomena of low-speed aerodynamics.

Boundary layer control (BLC), a method of achieving slow flight while maintaining high lift capability, proved promising to MSU and resulted in their application of this principle on several test aircraft (including a sailplane). This report presents the results of flight testing a modified Army L-19 aircraft with BLC installed and emphasizes the increase in take-off and landing performance gained through its usage.

The report is published for the exchange of information and the stimulation of ideas.

Task 1P125901A14203
Contract DA 44-177-AMC-265(T)
USAAVLABS Technical Report 66-36
June 1966

FLIGHT TEST EVALUATION OF A DISTRIBUTED SUCTION HIGH-LIFT BOUNDARY LAYER CONTROL SYSTEM ON A MODIFIED L-19 LIAISON AIRCRAFT

Aerophysics Research Report No. 66

by

Sean C. Roberts
Michael R. Smith
David G. Clark

Prepared by

The Aerophysics Department
Mississippi State University
State College, Mississippi

for

U. S. ARMY AVIATION MATERIEL LABORATORIES
FORT EUSTIS, VIRGINIA

ABSTRACT

A distributed suction high-lift boundary layer control system fitted to a standard liaison L-19 aircraft increased the aircraft C_L max to 5.74 and decreased the take-off and landing distance over a 50-foot obstacle by 38 percent and 29 percent, respectively, with no increase in available power. The modified aircraft demonstrated acceptable stability, control, and handling characteristics in all flight phases, and the stalling characteristics were good, with no rolling tendency. Considerable structural modifications were necessary to obtain the above results. The small holes in the boundary layer control system operated quite successfully for a period of 5 years without clogging due to dust or rain.

CONTENTS

ILLUSTRATIONS

SYMBOLS

c	wing chord, feet
C_{D_i}	induced drag coefficient
C_{D_o}	profile drag coefficient
C_f	flat plate skin friction coefficient evaluated at local Reynolds number
C.G.	center of gravity
C_L	aircraft lift coefficient
C_l	wing section lift coefficient
C_p	pressure coefficient
F_s	stick force, pounds
H	boundary layer parameter = δ^*/θ
q	dynamic head = $\frac{1}{2}\rho U^2$
q/q_o	ratio of local dynamic pressure to free-stream dynamic pressure
R_θ	Reynolds number based on the boundary layer parameter
THP_{ew}	thrust horsepower required
THP_{xs}	excess thrust horsepower available for climb
u	local velocity in the boundary layer, feet per second
U	local free-stream velocity, feet per second
U'	local velocity gradient in feet per second per foot
U_i	initial local velocity, feet per second
u/U	nondimensional boundary layer velocity
U_τ	skin friction velocity = $\sqrt{\tau_o/\rho}$, feet per second
U_∞	free-stream velocity, feet per second
V_{ew}	equivalent airspeed, miles per hour

V_o inflow velocity in feet per second

W_s standard aircraft weight

x distance measured parallel to the surface, feet

x/c nondimensional distance measured parallel to the surface, feet

y distance measured perpendicular to the surface, feet

δ boundary layer thickness, inches

δ^* boundary layer displacement thickness = $\int_o^\infty (1-\frac{u}{U})dy$, feet

δ^{**} boundary layer energy loss thickness = $\int_o^\infty \frac{u}{U}(1-(u/U)^2)dy$, feet

δ_e elevator angle of deflection, degrees

ΔP pressure differential, pounds per square foot

θ boundary layer momentum thickness = $\int_o^\infty \frac{u}{U}(1-\frac{u}{U})dy$, feet

θ' gradient of momentum thickness = $\frac{d\theta}{dx}$

θ_i boundary layer initial momentum thickness, feet

ν kinematic viscosity, square feet per second

η_p propulsive efficiency in level flight

η_{p_c} propulsive efficiency in climbing flight

ρ density of medium, slugs per cubic foot

τ_o surface shearing stress, pounds per square foot

CHAPTER 1. INTRODUCTION

For many years, aircraft designers have been attempting to decrease the minimum flying speed of fixed-wing aircraft to enable them to take off and land in short distances without incurring a severe drag penalty at high cruise speeds or requiring excessive horsepower. The attainment of such STOL characteristics is primarily dependent upon increasing the lifting capability of the aircraft wings. Many mechanical devices, such as flaps and slots, have been used to increase the maximum lift coefficient of an airfoil to 3.0, whereas high-lift boundary layer control systems have demonstrated a capability of achieving lift coefficients much greater than 3.0.

To prove effective, a boundary layer control system must not only increase the lift of the wings but also utilize sufficiently low horsepower to result in a net gain in take-off performance when the power for the system is taken from the main power plant. Also, the system must be mechanically simple, light, reliable, and easily maintained. A study by Cornish (reference 2) has indicated that the power requirements for a sucked or blown slot exceed the power requirements for distributed suction boundary layer control systems, with the result that a distributed suction boundary layer control system was chosen to increase the lifting capability of the test aircraft wings.

A distributed suction high-lift boundary layer control system was applied to a modified liaison L-19 aircraft, and this report gives the results of the flight evaluation of the modified L-19.

CHAPTER 2. DESCRIPTION OF MODIFIED L-19 AIRCRAFT

2.1. Background History of Project

In the early 1950's the Aerophysics Department of Mississippi State University was engaged in studying the biophysics of birds by means of trailing buzzards with sailplanes. Unfortunately, the sailplanes could not fly slowly enough to maintain formation with the birds, with the result that in cooperation with the Office of Naval Research, a project was initiated to decrease the flying speed and increase the lifting capability of sailplane wings. A Schweizer TG-3 sailplane was modified by punching numerous small holes on the upper surface of the wing, and suction was provided by four axial pumps which were battery powered. The result of these experiments was that the maximum lift coefficient of the unflapped wing was increased from 1.4 to 2.1.

In 1956, in conjunction with the Office of Naval Research and the U. S. Army Aviation Materiel Laboratories, an L-21 was modified to accept a boundary layer control system similar to that in the TG-3 sailplane. However, in this particular case, the suction air was passed along the inside of the wing through a double windshield and was used to cool the engine so that additional cooling was not required, and the engine air intakes were sealed. The pumps were mechanically linked to the engine, with the result that full boundary layer control was available for take-off at high engine r.p.m. but was not available for landing. This condition made the aircraft unsuitable for STOL landing performance, although it did demonstrate that aircraft lift coefficients of 4.2 could be obtained with the expenditure of approximately 10 horsepower from the engine. With the results of the above research being used as a guide, an L-19 aircraft was modified with a distributed suction high-lift boundary layer control system which could be utilized both for short take-off and for short landing.

2.2. Modified L-19 Aircraft

The third aircraft used in the STOL research program at Mississippi State University was a modified L-19 (Figure 1). A boundary layer control system similar to those of the TG-3 and the L-21 was installed together with pertinent modifications suggested by the previous research. Two hydraulically driven axial flow blowers, powered by a hydraulic pump at the main engine, were fitted to the aircraft, one under each wing (Figure 2). In this case, the boundary layer control could be varied independently of the engine speed, thereby making the system suitable both for the take-off and landing modes.

In the course of the research on this vehicle, it became necessary to perform certain modifications to increase the efficiency and safety of the operation in the STOL mode of the L-19 aircraft. The modifications are

listed below.

(a) To obtain adequate directional control at low forward velocities, the size and the shape of the vertical fin and rudder were altered, as shown in Figure 3.

(b) Small end plates were added to the horizontal stabilizer to increase elevator effectiveness at low speeds (Figure 4).

(c) The flap was modified so that attached flow could be maintained on the flaps without incurring a penalty of increased suction due to the severe adverse pressure gradient normally associated with sharp geometric discontinuities (Figure 5). The slot was eliminated because it was found that, even though the flow could be attached on the upper surface of the flaps, there occurred a separation of the flow in a very small area at the trailing edge of the wing which rapidly expanded into a large wake. It was found that the horizontal stabilizer lay in this low-energy flow so that the aircraft suffered from insufficient tail power with the slotted flap.

(d) End plates were attached at both ends of the flaps in an effort to decrease the induced drag associated with abrupt changes in spanwise loading (Figure 5).

(e) Fairings were added at the intersection of the lift strut and the bottom surface of the wing (Figure 6). It was found that, at high-lift coefficients where the front stagnation line is on the bottom surface of the wing, the flow from this stagnation line coming forward around the leading edge was being interfered with by the wing lift strut which in the L-19 is located at the 15-percent chord position on the bottom surface. The fairings effectively minimized the interference to the flow on the upper surface caused by the unfaired wing struts.

(f) As the turbulent boundary layer separation was suppressed at the trailing edge by suction boundary layer control and as higher lift coefficients were achieved, it was found that the condition of the laminar boundary layer at the leading edge became increasingly important. Because of the severe pressure gradients and the centrifugal forces involved in rounding a relatively sharp leading edge, local laminar boundary layer separation occurred and, when reattachment failed to occur, the loss of lift was quite abrupt. To overcome this condition, the leading edge was modified, as shown in Figure 7, to reduce the centrifugal forces and to maintain attached flow.

(g) During the course of the flight experiments, it was found that appreciable flow separation occurred on the aft canopy of the cockpit, which extends from the flap trailing edge to the fuselage. This flow separation, besides causing considerable drag increase,

was partially responsible for the loss in the effectiveness of the vertical stabilizer. The modified canopy shown in Figure 8 successfully eliminated gross flow separation down to the minimum flying speed of the aircraft.

2.3. Design of the Distributed Suction Boundary Layer Control System

The problem of designing the boundary layer control system can be divided into two parts: (1) the determination of the required suction flow quantity and its distribution and (2) the determination of the required suction pressure and the size of the holes. The amount and distribution of the porosity required for the wings of the L-19 were computed from the following von Kármán momentum equation:

$$V_o = \theta' + \frac{\theta U'}{U}(H+2) - \frac{1}{2}C_f U$$

The pressure distribution around an airfoil can be closely approximated by using the potential flow methods of Pinkerton and Theodorsen (references 8 and 11) so that the unknowns U and U' can be found if the angle of attack of the airfoil and the anticipated value of C_L are known. The value of H generally varies between 1.5 and 2.0 for a turbulent boundary layer, so that a value of $H = 1.8$ can be assumed and, due to its relationship in the above equation with other factors, any error in this assumption has a very small effect on the final result. To maintain attached flow, H must be less than 2.5 and θ must also remain reasonably constant. In the case of the L-19, R_θ has been kept constant, thereby making θ' easy to compute. The skin friction coefficient can vary over quite an appreciable range in a turbulent boundary layer with suction applied. An approach which has been reasonably successful is to assume that the impervious skin friction relationship is valid and can be calculated by using the relationship developed by Ludweig and Tillman (reference 7), which follows:

$$\left(\frac{U_\tau}{U}\right)^2 = 0.123\left(\frac{U\theta}{\nu}\right)^{-.268} 10^{-.678H}$$

Also, values of C_f can be obtained from the flat plate curves of C_f against Reynolds number. The latter method was used in the L-19 computations. The remaining unknown is the value of O_i at the position in the airfoil where suction begins. The value of O_i can be calculated from Tani's equation when the local velocity distribution around the airfoil is known:

$$\frac{\theta_i^2}{\nu} = 0.44\, U_i^{-6} \int_0^x U^5 dx$$

The total flow quantity requirements were found by an integration process of the local suction velocity distribution over the entire wing; and, together with the pressure differentials required for suction which were found from the external pressure distributions, a suction pump was designed for the system.

The porosity distributions calculated above must be applied to the wing in such a manner as to approximate the initial assumption of a continuous porous surface. This was performed by drilling rows of holes (.018 - .030-inch diameter), ten per inch, with the rows of holes separated no more than by the local thickness of the turbulent boundary layer. The size of the holes and the row spacing needed to achieve the required inflow velocity distribution were determined from the local pressure differential across the skin and from the porosity characteristics of the small holes drilled in the skin material. The porosity of the skin is a function of the material used and of the thickness of the skin, which must be determined from samples of the skin material prior to drilling the wing. Figure 29 gives the porosity distribution on the L-19 wing.

CHAPTER 3. PERFORMANCE

The total reduction in take-off distance to clear a 50-foot barrier was reduced by 38 percent through the use of distributed suction boundary layer control, and the landing distance over a 50-foot barrier was reduced by 26.5 percent. The maximum value of lift coefficient determined from the measurement of the stalling speed in the take-off configuration was increased from 2.86 to 5.74. The above increases in STOL performance were achieved even though the power required to drive the boundary layer control system was taken from the main power plant. The other items of performance, such as cruise flight and rate of climb performance for the modified high-lift L-19, were substantially unchanged over the standard L-19 liaison aircraft.

3.1. Take-Off and Landing

The take-off and landing performance was measured by means of a 35-mm movie camera with a telephoto lens which recorded the take-off and landing of the test aircraft from a position 500 yards from and perpendicular to the flight path. The ground run was posted at 50-foot intervals, and a 50-foot calibrated pole was erected at the end of the marked runway. The camera timing interval could be preset to any desired setting, depending upon the take-off characteristics of the aircraft. The results were corrected for parallax errors between the posts and the aircraft, and all data were reduced to a standard aircraft weight of 2,400 pounds and to standard atmospheric conditions. A typical series of L-19 take-off pictures is shown in Figure 9, and the results from these pictures are plotted in Figure 10 showing that a ground roll of 200 feet to 220 feet is required for the aircraft to become airborne and that a total of 420 feet is required to clear a 50-foot obstacle.

The minimum landing distance that was recorded without stalling the aircraft or indulging in any dangerous maneuvers was 580 feet over a 50-foot obstacle, which was 210 feet less than the minimum recorded at Edwards Air Force Base during the flight test of a standard L-19 (reference 10). The technique for obtaining minimum take-off and landing distances is described in paragraph 5.4 in the handling characteristics section.

3.2. Level Flight

The aircraft was instrumented with a calibrated and balanced airspeed and altimeter system, the engine r.p.m. and manifold pressure gauges were calibrated, and an angle of attack indicator and pitch meter were installed. Position error measurements were obtained by means of the trailing static sonde method. Figure 11 shows the variation of aircraft lift coefficient with equivalent airspeed, and Figure 12 shows the

relationship between C_L and angle of attack. From these curves it can be seen that C_L max = 5.7 at an aircraft airspeed of 30.0 miles per hour and an angle of 20 degrees with full flaps.

3.2.1. Power Required Tests

Level flight performance data obtained at a 2,000-foot pressure altitude are presented in Figure 13. The results have been corrected to standard conditions and an aircraft weight of 2,300 pounds. All level flight performance was obtained with the hydraulic motor driving the boundary layer control system in operation. The minimum power required to fly the modified L-19 with flaps up is 75 brake horsepower at an airspeed of 67.5 miles per hour. It is interesting that at low speeds, i.e., below U_∞ = 45 miles per hour, the horsepower required to fly with 15 degrees of flaps is less than that required to fly with no flaps. This can probably be accounted for by a possible reduction in induced drag with 15 degrees of flaps due to changes in the spanwise loading of the wings at high aircraft lift coefficients. The power required to fly at the minimum airspeed of 30 miles per hour is 154 brake horsepower, which is a considerable portion of the horsepower available from the engine.

3.2.2. Glide Tests

Free-flight glide tests were employed to determine the drag coefficient and thrust horsepower required to fly the aircraft in the absence of propeller interference. In these tests, the propeller of the aircraft was removed and ballast added by attaching a flywheel to the aircraft and by using properly positioned lead weights to maintain a gross take-off weight of 2,300 pounds and a midrange C.G. position. The reason for attaching the flywheel on the propeller shaft was to enable the aircraft engine to be run in flight up to an r.p.m. of 1,700 so that the boundary layer control system would be operating for the slow flight configuration. The aircraft was towed to a maximum altitude of 6,000 feet, to prevent overloading the suction pumps, and was released and flown back to the air base at various stabilized airspeeds. The rate of sink was recorded, from which the thrust horsepower required to fly the aircraft at a given speed was computed by equating the change of potential energy to the kinetic energy. Figure 14 shows the results of the glide tests. From these curves, it is increasingly obvious that the power required to fly at low airspeeds is considerably reduced when flaps are used instead of the unflapped wing. This could be due to the decrease in profile drag with sealed flaps and to the considerable reduction in the pressure gradients on the upper surface of the wings. Therefore, the boundary layer thickness with a constant boundary layer control suction would probably be less than that associated with an unflapped airfoil. Also, the changes in spanwise loading with the application of flaps would affect the induced drag of the wing.

3.3. Climb Performance

The rate of climb performance was investigated to determine that the addition of the boundary layer control system had affected the operational characteristics of the aircraft other than the take-off and landing modes. Sawtooth rate of climb tests were performed by obtaining a plot of altitude against time for various aircraft airspeeds and flap settings at a mean altitude of 1,200 feet. The data were corrected to standard sea level conditions for a standard aircraft weight of 2,300 pounds, and the results are presented in Figure 15. A maximum rate of climb of 1,250 feet per minute at an airspeed of 70 miles per hour agrees very well with the results of the unmodified L-19, where the rate of climb was 1,270 feet per minute (reference 10).

The excess horsepower available for climb was also computed, and the results were added to the power required for level flight, as shown in Figure 16. From these curves, estimates of the propulsive efficiency in the climb were calculated and added to Figure 16.

CHAPTER 4. STABILITY AND CONTROL

In the design of the boundary layer control system, the aircraft not only must have the capability of flying at very high lift coefficients but it also must have sufficient static and dynamic stability and control power to enable a pilot to fly the aircraft safely in the STOL mode of flight during take-off and landing and in turbulent air. From the initial flight tests, it was obvious that ample lateral control was available at all speeds down to and through the complete aircraft stall with boundary layer control applied to the ailerons. Longitudinal control was sufficient except with full flaps and zero power settings and at low airspeeds where round-out to the three-point altitude in landing was marginal. This was not a problem when the propeller was on the aircraft, as sufficient engine r.p.m. had to be maintained to assure full boundary layer control so that the elevator power available was ample at all settings. However, when the propeller was removed, the maximum C_L that could be achieved was 2.4 because of insufficient elevator power to rotate the aircraft. Small end plates, as described in paragraph 2.2, were added to the elevator to improve control effectiveness.

Directional control was marginal at low airspeeds just prior to take-off or in the landing phase with any crosswind; to overcome this problem, the vertical stabilizer area was increased as described in paragraph 2.2. Since the major effect of a distributed suction boundary layer control system on the stability of an aircraft would be felt in the longitudinal phase, the flight tests were concentrated on the stick-fixed, stick-free, static longitudinal mode. Qualitative checks on the lateral and directional modes and on the dynamic stability of the modified L-19 have been thoroughly investigated by previous investigators.

4.1. Longitudinal Stability

Stick force and elevator angle as functions of aircraft airspeed were measured on the modified L-19 both for the zero flap conditions and for the full flap conditions at three C.G. positions. These curves are presented in Figures 17 and 18. Also, a curve of stick force against flap angle holding a constant trim speed is shown in Figure 19. The stick force results (Figure 17) show that a 20-pound stick force is required to reduce the airspeed from the cruise to minimum flying speed with the flaps up; however, if full flaps are applied without retrimming as the aircraft airspeed decreases, the maximum out-of-trim stick forces are reduced to +9 pounds. The elevator angle results indicate that the effect of the flaps is to change the downwash angle so that down elevator is required to trim the aircraft. This effect is obviously larger than the rearward motion of the center of pressure normally associated with the application of flaps.

Longitudinal control was adequate in all conditions with boundary layer control, since sufficient engine r.p.m. had to be maintained to

provide boundary layer control in order that the propeller slipstream velocities were sufficient to ensure that the elevators were quite effective. Problems arose only when the propeller was removed for gliding flight, and this would not be considered to be normal operating practice. The effect of power changes on trim for the overshoot case when operating in the STOL mode, for instance, U_∞ = 40 miles per hour, was considerable as the stick force changed from +5 pounds (pull) in the landing mode to -8 pounds (push) at full throttle. Aircraft airspeeds below 60 miles per hour were unobtainable with flight idling power, as the boundary layer control system was lost and the aircraft stalled.

The minimum trim speed of the aircraft at the 27.0-percent C.G. positions is 45 miles per hour with no flap and 34 miles per hour with full flaps.

The dynamic stability of the modified L-19 did not have any unusual characteristics; the aircraft demonstrated good dynamic longitudinal characteristics, with the controls fixed or free, for both positive and negative changes in pitch induced by the elevator.

4.2. Lateral and Directional Stability

Steady sideslips with full flaps at low airspeeds could be accomplished only up to sideslip bank angles of 5 degrees before running out of rudder effectiveness. Aileron control characteristics in the sideslip were acceptable with positive roll control down to the stall speed in all aircraft configurations. Considerable adverse yaw was evident in slow-speed flight; however, the additional fin area on the modified L-19 resulted in better directional stability characteristics than the standard L-19 at the same airspeeds. Directional control was adequate in all flight configurations; however, in the STOL mode of operation, when the tail is raised to aid in the acceleration of the aircraft at speeds of 20 miles per hour, the rudder power is just sufficient to overcome torque effects and is inadequate to overcome any lateral wind component. Therefore, it is recommended that optimum short take-off be performed directly into the wind. Short landing presents the same problem of marginal directional control at low power settings, and the pilot must use large rudder inputs to correct deviations from the path of flight.

The dynamic lateral-directional stability is very good in all configurations tested, including the low-speed phase, with the oscillations appearing to be critically damped.

CHAPTER 5. HANDLING QUALITIES

5.1. Stick Forces and Control Response

The longitudinal stick forces on the L-19 require continual retrimming if any of the variables such as flaps or power are used from one extreme to the other. Under these conditions, when approaching at flight idling with full flap, the application of power requires considerable stick forces to maintain airspeed. Also, the elevator forces cannot be trimmed out with full trim. With this in mind, it is very necessary when flying the modified L-19 that the aircraft be trimmed for the proper take-off prior to flying, as the elevator stick forces required to maintain the flight speed may be quite excessive and beyond the capabilities of the average pilot to hold. The longitudinal elevator control response is adequate for all flight conditions except those at very low airspeeds, i.e., at aircraft lift coefficients greater than 4.5. It has been found, however, that insufficient elevator power is available if the engine is not operating at high r.p.m.'s. For example, during the glide test when the propeller was removed, the maximum lift coefficient that could be obtained with the aircraft was equivalent to an airspeed of 48 miles per hour, and the reason for the relatively low maximum lift coefficient of 2.3 was due to having insufficient elevator power to rotate the airplane; i.e., the maximum lift coefficient of the aircraft was governed by the elevator movement and the control effectiveness of the longitudinal controls. The lateral and directional control forces are within operational limits of this aircraft through all flight airspeed ranges; however, at very low forward velocities at lift coefficients greater than 4.5, adequate directional control is marginal unless high power settings are on the engine, whereby the slipstream artificially increases the control effectiveness of the rudder.

5.2. Stalling Characteristics

Stall warning is inadequate in that stall buffet is slight and occurs only at approximately 1 to 2 miles per hour higher than the stall speed even in the high-lift STOL mode of flight. The complete stall in the STOL mode is mild, and rolling does not usually occur. Recovery is made by decreasing the backward pressure on the stick, and the aircraft can be recovered generally in less than 100 feet. A sharp forward motion of the stick unloads the wings by means of the centrifugal forces applied to the aircraft, and flow reattachment is quite rapid. Recovery from accelerated stalls is accomplished by a forward movement of the stick; however, if sideslip is present in these accelerated maneuvers, considerable wing drop occurs and much altitude can be lost before recovery is accomplished. As can be seen from Figure 20, the stall in the high-lift condition generally starts at the outer edge of the propeller slipstream. Obviously, the outer edge of the propeller slipstream disturbs the flow sufficiently to promote a thick boundary layer and

premature separation. During the stall maneuvers, the separated flow spreads very quickly from the region of the outer edge of the propeller slipstream, and complete stall can occur in probably less than 1 second, thereby requiring a quick response by the pilot to prevent catastrophic results. It is recommended that in an L-19 with a high-lift boundary layer control system, a stall warning indicator which is independent of flap angle, weight, power setting, and accelerated maneuvers be used.

5.3. Slow Flight Characteristics

When the L-19 is in the STOL mode of flight with the flaps up, i.e., at an angle of attack greater than 35 degrees, the forward visibility of the pilot is greatly restricted. However, when flying at 1 or 2 miles per hour above the stall speed, the control response is adequate in all three axes of flight. It will be noticed, however, that sideslips cannot be accomplished in the STOL mode either with or without flaps when the airspeed is less than 40 miles per hour. This is due to inadequate rudder effectiveness to hold a straight flight path at bank angles greater than 5 degrees. Therefore, it is necessary to rule out the sideslip approaches in combination with a high-lift boundary layer control system for a steep landing approach technique. Besides being difficult to see out the front while flying in turbulent air in the STOL mode of flight with no flaps, it is extremely difficult to maintain proper attitude control. A similar condition occurs with the full flaps, as attitude is difficult to control and there is very little aerodynamic stall warning; thus, continual monitoring of the airspeed indicator is required. Also, as the aircraft is flying on the backside of the drag curve, which means that the aircraft is speed unstable in the STOL mode, considerable power changes are required to maintain either a constant airspeed or a constant angle of flight path. These conditions make it very difficult to fly this STOL aircraft accurately in turbulent air at lift coefficients greater than 3.5.

5.4. Short Take-Off and Landing Techniques

The shortest distance to clear a 50-foot obstacle can be obtained by taking off with full flaps and full throttle - with full throttle being applied prior to brake release. The technique is to raise the tail off the ground as soon as possible by releasing the brake and applying full forward stick. The tail lifts at approximately 15 miles per hour and aids the acceleration to the lift-off speed of 33 miles per hour; rotation is accomplished to maintain a constant airspeed of 35 miles per hour, which is the climb-out speed to clear a 50-foot obstacle. During the ground run, full right rudder is normally required to maintain a straight ground path up to speeds of at least 25 to 30 miles per hour. If rotation is attempted prior to obtaining minimum flying speed, the tail drags on the ground and thereby prevents the proper angle of attack on the airfoil being obtained, and the aircraft will considerably

extend its take-off ground run above normal operation. Even in the optimum take-off condition, the tail wheel will touch the ground and will be the last thing to leave the ground; however, if flying speed is obtained before this happens, the aircraft will rotate and climb out. In crosswind conditions, insufficient rudder power is available to correct drift if the crosswind is from the left and is greater than 5 miles per hour. Therefore, it is recommended that STOL approaches not be made in crosswind conditions unless the tail wheel is kept on the ground until the airspeed reaches at least 30 miles per hour, which would, of course, considerably extend the ground run beyond the optimum.

Short landings are extremely difficult to perform in the modified L-19 aircraft, because in the STOL mode, forward visibility is very bad at high angles of attack. The addition of full flaps alleviates this problem somewhat. However, as the approaches are quite steep, it is extremely difficult to see forward when clearing a 50-foot barrier, and slight sideslip of a few degrees to achieve visibility out the side is required for accurate flying. The necessity of having high power settings to obtain high-lift coefficients, since the boundary layer pump is directly connected to the main engine, means that the rate of sink of the aircraft is relatively low, and considerable float will occur over a 50-foot obstacle. Partial stall approaches can be performed whereby the aircraft is partially stalled, by a reduction of power on top of the obstacle, and is recovered prior to touchdown on the ground. This kind of approach is very marginal in safety and is not recommended. Minimum distance landings have been obtained through the use of a steep gradient approach started at 200 to 300 feet and flown at 40 miles per hour. Just prior to landing, the airspeed is decreased and a burst of power is employed from the engine to effect round-out. It is necessary that the throttle be closed immediately after the burst of power to reduce floating to a minimum. This technique requires careful judgement and considerable practice, as delay in application of power results in a tremendous landing load on the undercarriage and, with the application of power, considerable floating down the runway. Premature application of power and rotation also extends the floating beyond the acceptable limits. However, when the aircraft touches the ground at about 35 miles per hour and the throttle is closed, there is no tendency for the airplane to do anything but stop, as the aircraft is fully stalled; and with the application of the brakes, the aircraft can be stopped in a very short distance.

5.5. Acceleration Technique Between High-Lift and Conventional Flight

Of considerable interest to the operational pilot of a STOL airplane is the time required to accelerate the aircraft from its STOL condition to the conventional straight flight condition and the time and technique required to slow the aircraft down from the conventional to the STOL mode of flight. The modified L-19 after a STOL take-off with full flaps and power can be accelerated quite rapidly by maintaining full power, and by leveling off and retracting the flaps. Fortunately, the

flap position control is close to the propeller pitch mechanism which must be monitored as the airspeed increases; nevertheless, this requires the pilot to stop the retraction of the flaps while he adjusts the prop pitch control. It is recommended that in this type of operation the flaps have a switch that operates continuously and that the pilot preset the position desired, thereby eliminating the continuous presence of his hand on the switch during operation. The time required to perform this operation can generally be decreased somewhat if the aircraft is allowed to dive slightly to help accelerate the aircraft to maximum forward velocity.

In the reverse phase, transitioning from normal conventional high-speed flight to the STOL mode requires the following operation: the application of carburetor heat, the reduction of the throttle to flight idling, and the rotation of the airplane to maintain a constant altitude. As the aircraft airspeed decreases below the maximum flap angle airspeed condition, flaps are continuously applied. As the airspeed continues to decrease and the power required for level flight increases with large applications of flap, the throttle must be reapplied to maintain level flight conditions. This requires considerable dexterity and practice of the pilot to perform these operations skillfully and smoothly. Similarly, it would be nice if the flap could be preset to the full-down condition, thereby eliminating the presence of the pilot's hand on the flap actuator so that he could more usefully employ that hand in applying the power to maintain level flight. The time to accelerate the aircraft from the STOL mode requires 21 seconds, and the time required to decelerate from conventional flight to minimum flying speed in the STOL mode is 23 seconds; a constant altitude is maintained throughout the transition.

5.6. Boundary Layer Control System Failure

If the boundary layer control system on this high-lift STOL aircraft fails in the STOL phase, then, of course, the aircraft will be completely stalled. If this should occur, it would be of interest to the pilot to know the minimum altitude that is required so that control of the aircraft can be regained prior to contact with the ground. A simulated boundary layer control system failure was attempted in flight at 3,000 feet, both with the aircraft in the STOL mode at minimum flying speed with no flap condition at an aircraft angle of attack of 28 degrees and also with the full-flap condition and a minimum flying speed of 31 miles per hour. To simulate a complete failure, the engine was decreased to flight idling, the aircraft was stalled, and the altitude required to regain sufficient flying speed to flare the airplane was determined by a chase plane and long-range photographic cameras and also by recorded instrumentation in the cockpit of the L-19. When the throttle was retarded to flight idling, the aircraft immediately stalled; however, the stall was quite mild and the aircraft pitched forward with no tendency to roll off to either side. The stall was quite complete, and the aircraft in the

flaps-up condition rotated from an attitude to the ground of 30 degrees nose-up to approximately a 60-degree nose-down angle. However, in this condition with the flaps up, airspeed was regained quite rapidly and the aircraft rounded out with a maximum altitude loss of 250 feet. In the full-flap condition, the aircraft stalled very abruptly and rotated round through a pitch angle change of approximately 60 degrees. The aircraft airspeed increased quite rapidly, and the aircraft was able to be rotated at an approximate airspeed of 60 miles per hour. The limiting factor in this case was the elevator control effectiveness required to rotate the airplane; also, in the full-flap condition the aircraft could be rotated and flared so that it would contact the ground or land on the ground so long as the complete system failure occurred at an altitude greater than 230 feet above the surface. It is obvious from this result that in STOL operation, if a power system failure occurred in a single-engine STOL aircraft below an altitude of 250 feet, the pilot would have considerable difficulty in getting out of the airplane; and as the attitude changes are so extreme, even an ejection might put the pilot in a hazardous position. It is therefore obvious that the STOL mode of operation should not be performed below 250 feet above the ground except during the take-off and landing phases. To recover from the stall, a small forward application of the stick is required to increase the airspeed and then a full backward motion of the stick is required to round the aircraft out prior to contact with the ground. Throughout this whole operation, adequate directional and rolling control was available; however, it was not needed, as the aircraft did not have a tendency to drop a wing so long as the aircraft was in straight and level flight.

CHAPTER 6. AERODYNAMIC DATA

6.1. Airfoil Pressure Distributions

The pressure distributions on a high-lift wing at high-lift coefficients are of interest to the aerodynamicist who must predict a pressure distribution from potential flow theory to enable him to design the distributed suction boundary layer control system. This being the case, it was necessary to measure the pressure distributions on the high-lift wing of the L-19 and, if possible, to compare them with the theoretical pressure distributions that were predicted by the theories of Theodorsen and Pinkerton. The pressure distributions were measured on a section of the port wing 50 inches from the wing root. A pressure tape consisting of 20 multitube polyethylene tapes was attached to the upper and lower surfaces of the wing, and holes were drilled in the tape at positions where the pressure reading was required. A vast majority of the pressure tapes were located on the upper forward section of the airfoil, where the pressure gradients can be quite severe and pressure peaks occur at about the 5-percent chord position on the wing. The tapes were then routed to the rear cockpit of the L-19 and attached to a large multitube photomanometer which could be filled either with water or with tetrachloride. Figure 21 shows the arrangement of the manometer in the back cockpit of the L-19. To correct for differences in angle, an inclinometer was attached to the manometer so that when the aircraft was at high angles of attack, the manometer readings could be corrected for this angle of inclination.

Pressure distributions were recorded over the wing section at various aircraft airspeeds and flap settings. Figure 22 shows a series of measured pressure distributions that were calculated from the manometer readings by use of a digital computer. These pressure distributions show the effect of airspeed on the local pressure distribution for the full-flap case. Figure 23 shows the effect of flap angle on the pressure distribution of the L-19 for constant indicated airspeed. The pressure distribution curves were integrated by means of digital computer techniques and the local sectional lift coefficients obtained and recorded on each pressure distribution chart.

The pressure distributions given in Figure 22 clearly show the very high pressure peak associated with airfoils at high angles of attack with distributed suction boundary layer control. In the case where the sectional lift coefficient is 4.29, the minimum pressure coefficient reaches a value of minus 26.0. The pressure peak creates many problems in that it is a major factor in laminar boundary layer separation prior to the beginning of the distributed suction boundary layer control. Also, the pressure differences required of the pumps to ensure inflow at these low pressure coefficients make the design of the pump difficult. The flap section of the wing contributes quite significantly to the lift coefficient. This is clearly shown where the airspeed is relatively large,

i.e., 45 miles per hour, where the shape of the pressure distribution curve shows the bulge at the rear. This low pressure region at the rear of the airfoil ensures that for a constant wing lift the pressure gradients on the wing are much lower than they normally would be with an unflapped airfoil at a large angle of attack. The effect of the power from the engine on the aircraft lift coefficient is very significant and can be clearly seen if the section lift coefficient is compared with the aircraft lift coefficient for any particular curve. When the angle of attack is high, i.e., when the free-stream velocity is low, the difference is approximately 1.4. For example, at an airspeed of 31 miles per hour, the aircraft lift coefficient is 5.7, whereas the maximum local lift coefficient on the flapped wing is 4.3; these figures indicate that a considerable thrust increment is off-loading the wings. The difference between the aircraft lift coefficient and the local section lift coefficient decreases as the aircraft airspeed increases or as the angle of attack of the airfoil decreases, which would be expected.

The effect of flaps on the shape of the pressure distribution at a constant aircraft lift coefficient was primarily to decrease the minimum pressure peak that occurred on the airfoil. For example, at the 0-flap position, the minimum C_p was -16.0 (Figure 23); whereas, at the same aircraft lift coefficient at full flaps, the minimum pressure coefficient was -12.0. This is a very important effect with regard to the design of the pumps required for a distributed suction boundary layer control system, which indicates that for the high-lift condition, full flaps or a highly cambered airfoil section should be used in the high-lift STOL mode of flight. A variation in the local section lift coefficient with regard to various flap angles was very small, the maximum variation being less than 8 percent, varying from 2.84 at 0-flap to 3.05 for the full-flap case.

6.2. Boundary Layer Measurements

Boundary layer profiles were measured on the upper surface of the wing in the chordwise direction at all airspeed and flap positions. The probes on the wing were multichannel, total head tubes with an attached static tube; the total head tubes were in a vertical line to overcome the possible error associated with local spanwise differences in the boundary layer flow. Figure 24 shows the boundary layer probe. The boundary layer profiles were recorded on a multitube manometer; polyethylene overlay sheets and a grease pencil were used to record the information. A series of boundary layer profiles is shown in Figure 25.

By means of a digital computer, the boundary layer quantities δ^*, δ^{**}, θ and the parameter H were calculated for each boundary layer profile; and plots of δ^*, θ, and H against x/c for the two main flap conditions of zero flap and full flaps were made.

The series of boundary layer profiles clearly show the thickening of the boundary layer across the chord of the wing; and at one position,

namely, the 50-percent chord position, an inflection point appears in the profile indicating possible imminent separation. This 50-percent chord position corresponds to a 3-inch gap in the porosity of the upper surface of the wing owing to a spar position. The sudden loss in energy of the boundary layer at the 50-percent chord position with full flaps can be seen from the increase in loss of momentum thickness shown in Figure 26. This critical point in the boundary layer at the 50-percent chord position is not observed in the no-flap case, where the pressure gradient without flaps is not as severe as in the full-flap case where higher section lift coefficients are achieved. The increase in porosity aft of the impervious section of the wing was sufficient to suppress the imminent boundary layer separation. The growth of the boundary layer in the zero-flap condition, as evidenced by the parameters plotted in Figure 27, shows the controlled growth of the boundary layer associated with maintaining a constant R_θ in the boundary layer theory in designing a distributed suction boundary layer control system.

6.3. Boundary Layer Control System

The two blowers mounted under each wing of the modified L-19 to provide the suction for the boundary layer control system are hydraulically driven from a hydraulic pump which is directly driven from the main power plant. The pump was designed such that full output was available for boundary layer control at all engine r.p.m.'s greater than 1700 r.p.m. Figure 28 shows the variation of wing internal pressure as a function of engine r.p.m., and it can be seen that above 1700 r.p.m. the wing internal pressure is constant. This means that full boundary layer control is available at relatively low power settings for the landing phase of operation, which should assist in short landings. The hydraulic system operates at 3,000 p.s.i.; and to ensure that the hydraulic pump is always primed, the hydraulic fluid reservoir is pressurized to 25 p.s.i. by air.

The porosity distribution calculated using the techniques described in paragraph 2.3 and flight tested on the L-19 is shown in Figures 29 and 30. Figure 29 shows the row spacing on the upper surface of the wing and the diameter of the holes. The holes were drilled in rows, with 10 holes per inch, by a pneumatically operated drilling machine which could drill 40 holes per minute as it progressed along a rail on the surface of the wing. Figure 30 shows the cumulative porosity of the L-19 wing. Figure 31 shows the drilling machine used to obtain the porosity.

6.4. Wing Wake Interference at the Tailplane

It was found that, with the original L-19 wing which had a slotted flap, even though the flow could be attached to the flap, there occurred a separation of the flow in a very small area at the trailing edge of the wing which rapidly expanded into a large wake. Figure 32 shows the

details of the flow in a slotted flap where the boundary layer on the lower wing surface passing through the slot separates at point A, giving rise to a layer of low-energy air between the flow attached to the flap and the free-stream flow. Figure 33 clearly shows the separated flow region on the L-19 by means of tufts on a rake; the detrimental effect that this low-energy air would have on the tailplane effectiveness if the tailplane at any time operated in this region is indicated.

To overcome this problem of large wakes and also to ease the difficulty of providing suction to a separated flap section, the slot flap was modified to a sealed flap as shown in Figure 5. The dynamic head at the tail of the L-19 was measured by means of a wake rake as shown in Figure 34, and typical plots of the result at various aircraft airspeeds and lift coefficients are drawn in Figure 35. The survey at the horizontal tailplane indicates that the horizontal stabilizer is at the optimum vertical position that gives relatively high dynamic head for all flap and engine settings. Displacement of the horizontal stabilizer either up or down would result in decreased tailplane effectiveness, either at zero flap settings or at full-flap settings in the high-lift configuration.

6.5. Aircraft Drag Analysis

By utilizing the information obtained from the glide tests and level flight tests, it is possible to determine basic aerodynamical data such as the minimum aircraft profile drag coefficient, the maximum efficiency of the wings, the effective aspect ratio, the propulsive efficiency, and an estimate of interference drag.

Propulsive efficiency is defined as the ratio of power required to brake horsepower generated by the aircraft engine; as such, it is not a measure of propeller efficiency, since it includes losses due to engine cooling and interference drag. The propulsive efficiency of the test aircraft in level and climbing flight is presented in Figure 16.

The linearized drag polar for the test aircraft in gliding flight is presented in Figure 36. Extrapolation of the curves to the $C_L = 0$ line indicates that the minimum profile drag coefficient of the vehicle is 0.042 and 0.083 for the 0^o flaps and 40^o flaps configuration, respectively. A drag analysis for the two preceding configurations is presented in Figures 37 and 38. The induced drag coefficient was computed on the basis of the effective aspect ratio listed in Figure 36. The unusual shape of the aircraft profile drag coefficient in Figure 37 is due to the fact that the aircraft must fly at unusually high angles of attack at low speeds. At speeds greater than 75 or 80 miles per hour, the boundary layer control system is able to maintain an almost constant wing profile drag coefficient, and the reduction in angle of attack of the fuselage with increases in forward speed effects a reduction in fuselage drag coefficient. These two factors offset one another in the speed range between 80 to 125 miles per hour, as is evidenced by the constant

aircraft profile drag coefficient shown in Figure 37. A similar interaction occurs in the 40° flaps configuration (Figure 38).

The profile drag of the aircraft wing was measured in level flight to determine the variation of the profile drag coefficient with airspeed. The profile drag was determined by measuring the velocity distribution in the wing wake with a remotely controlled traversing probe which measured the dynamic and static pressure at each data point (Figure 39). The profile drag was then determined by graphically integrating the velocity distributions. The results of these measurements are presented in Figure 40.

6.6. Wing Tip Vortex Investigation

To determine the shape, approximate velocities, size, and movement of the wing tip vortices shed from the wing of the L-19 at high aircraft lift coefficients, a series of tests using the dust bomb technique were performed (reference 9). Briefly, the dust bomb technique consists of injecting a small quantity (1/2 pound) of finely granulated dust or powder into the wing tip vortex by means of a small, flat box attached to the underside of each wing tip. The entrainment of the dust into the vortices and the movement of the vortices in ground effect can be photographed, with telephoto lenses from the ground at the rear of the aircraft. Sequence pictures, photographed with a 35-mm camera with automatic rewind and an intervalometer, give a time scale on which can be plotted the vertical and horizontal movements of the wing tip vortices. Figure 41 is a plot of the results obtained from the photographs and shows the vertical and lateral movement of the vortex cores.

CHAPTER 7. CONCLUSIONS

The effect of adding a distributed suction boundary layer control system to a standard liaison L-19 aircraft resulted in appreciable changes in take-off and landing performance with the same available power plant; i.e., 38 percent decrease in take-off distance and 29 percent decrease in landing distance. The modified aircraft demonstrated adequate stability and control characteristics in all flight phases; the stalling characteristics were good, with no tendency for either wing to drop; and acceptable aileron control was available down to and through the stall. System failures, either in the blowers or in the engine, when operating in the STOL mode, resulted in complete aircraft stall; however, by off-loading the wings by prompt forward motion of the control stick to regain airspeed, the aircraft could then be flared for a landing in the 3-point attitude with a maximum altitude loss of 250 feet. Adverse roll characteristics associated with the loss of one wing blower are alleviated by a crossover duct in the boundary layer control system between the wings. The decreases in cruise performance were negligible, i.e., less than 3 miles per hour, with the boundary layer control system off.

In the STOL mode of operation, the aircraft is flying on the back-side of the drag curve which means that the aircraft is speed unstable; considerable changes in power setting are required to maintain either a constant airspeed or a constant angle of flight path. These conditions make it very difficult to fly this STOL aircraft accurately in turbulent air at lift coefficients greater than 3.5.

To accomplish the above increases in performance, considerable modifications, such as the following, were made to the aircraft: sealed flap, drooped leading edge radius, hydraulic pump installation, increased vertical stabilizer area, end plates on flaps and elevators, and modified aft canopy. The small holes drilled in the upper surface of the wing did not suffer from blockage effects due to dust or rain over a 5-year period of flying and exposure to the natural elements. The increase in the basic weight of the aircraft due to the modifications was 188 pounds.

Due to the extensive modifications that had to be made on the L-19, it is not recommended that distributed suction boundary layer control systems be retrofitted to existing aircraft. If true STOL performance is required, together with acceptable stability as well as control and handling characteristics, it is recommended that the boundary layer control system be incorporated in the initial design stages.

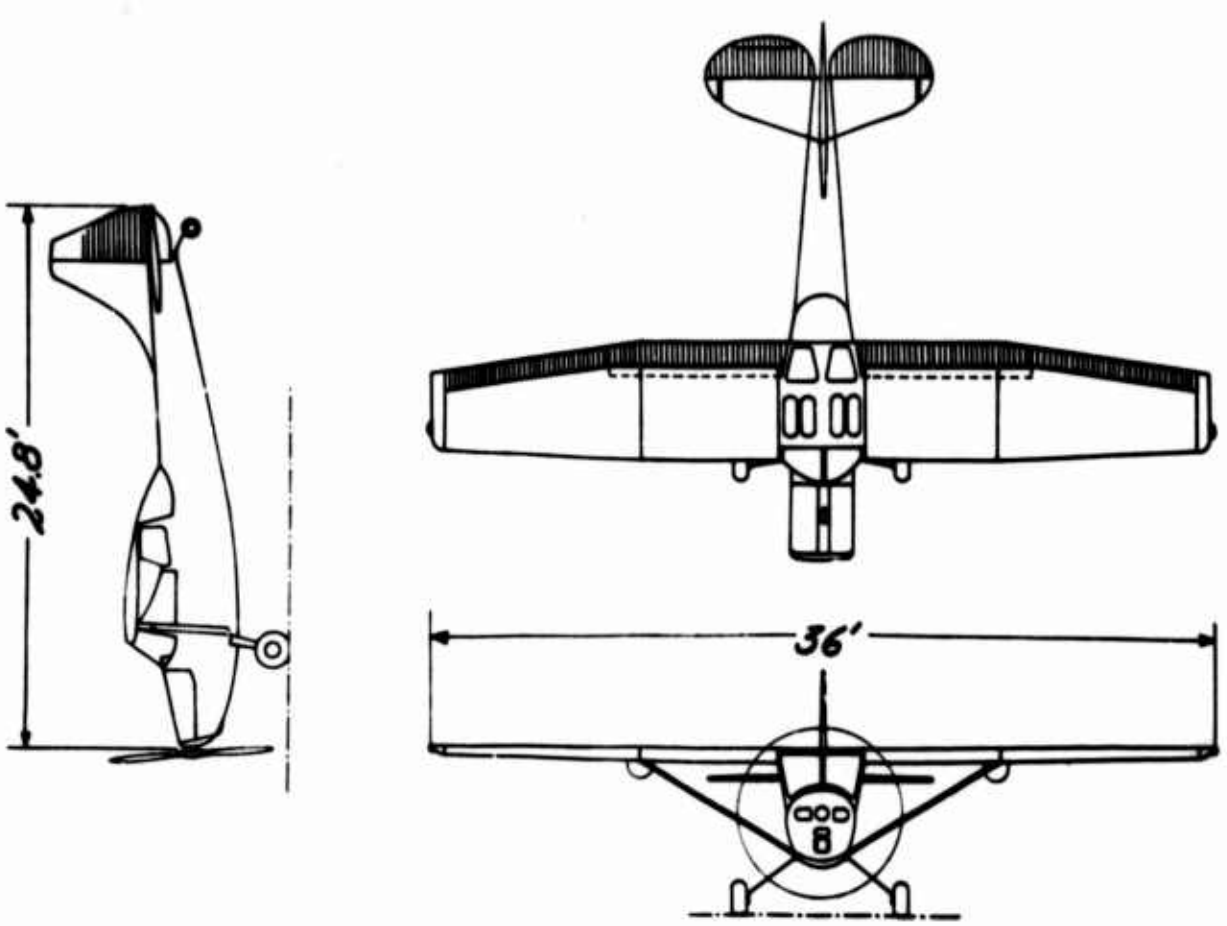

Figure 1. Modified Cessna L-19 High-Lift Research Aircraft.

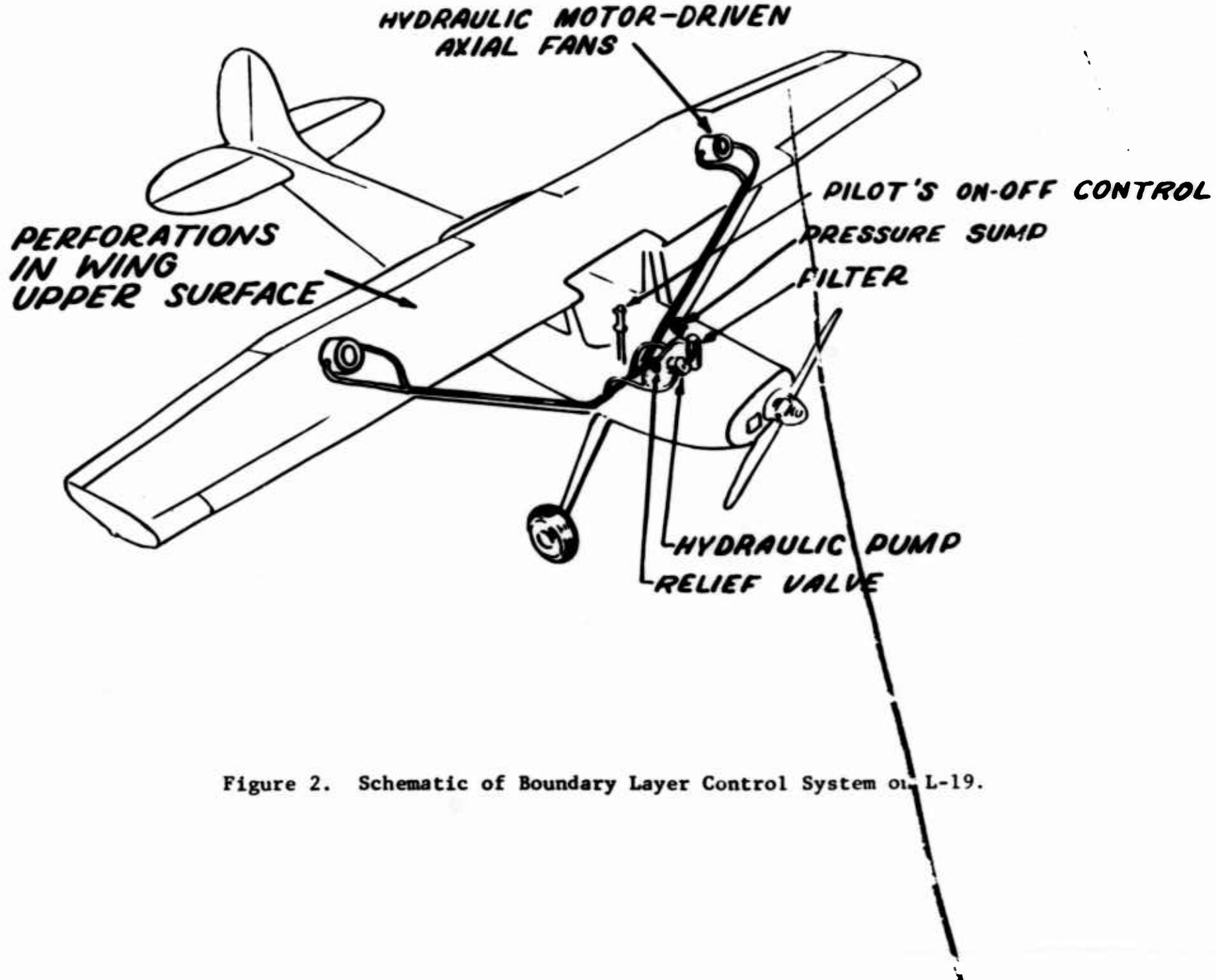

Figure 2. Schematic of Boundary Layer Control System on L-19.

Standard L-19

Modified L-19

Figure 3. Modifications to the Vertical Fin and Rudder of L-19.

Standard L-19

Modified L-19

Figure 4. End Plates on Horizontal Stabilizer.

Standard L-19

Modified L-19

Figure 5. Modified Flaps of L-19.

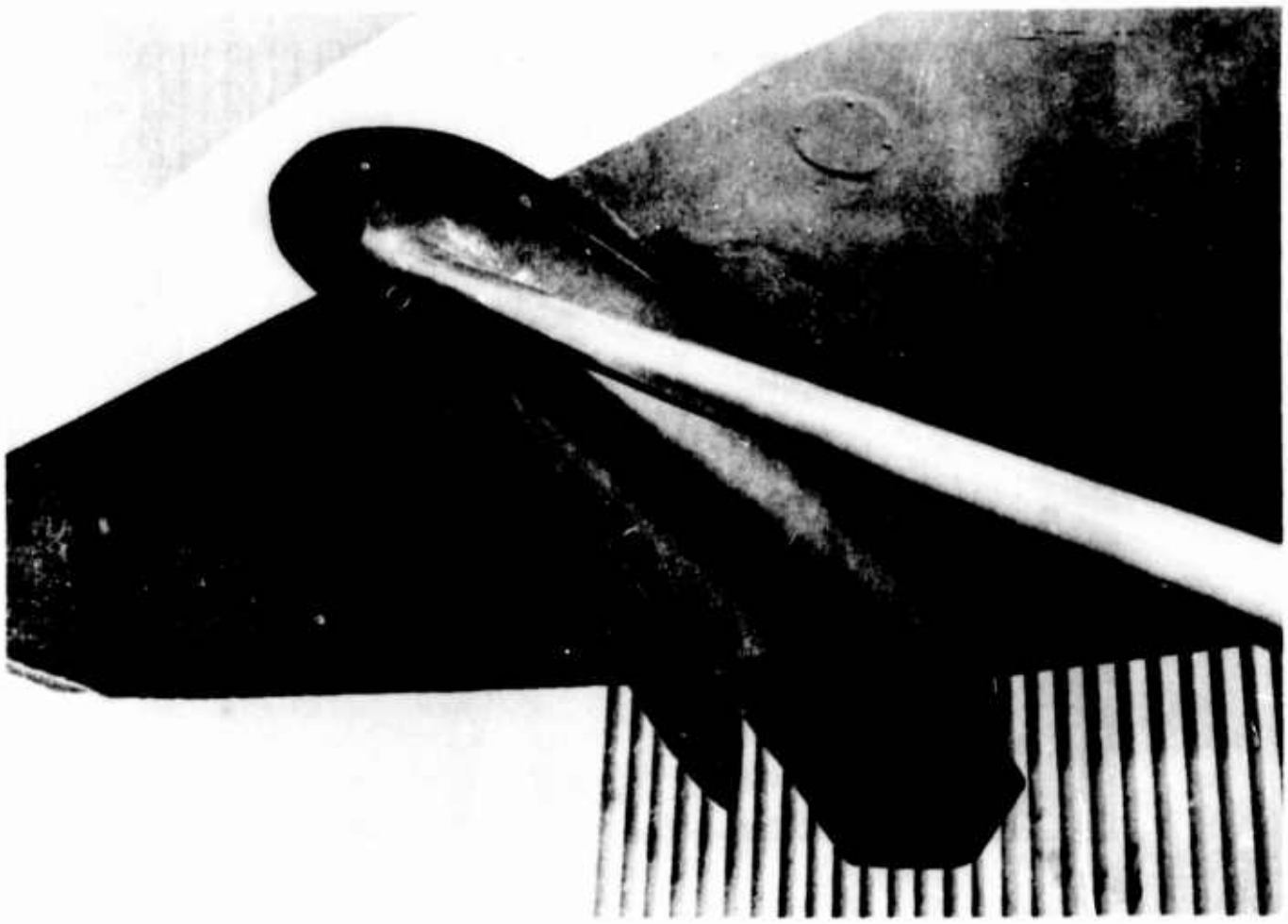

Figure 6. Fairing at Lift Strut and Wing Intersection.

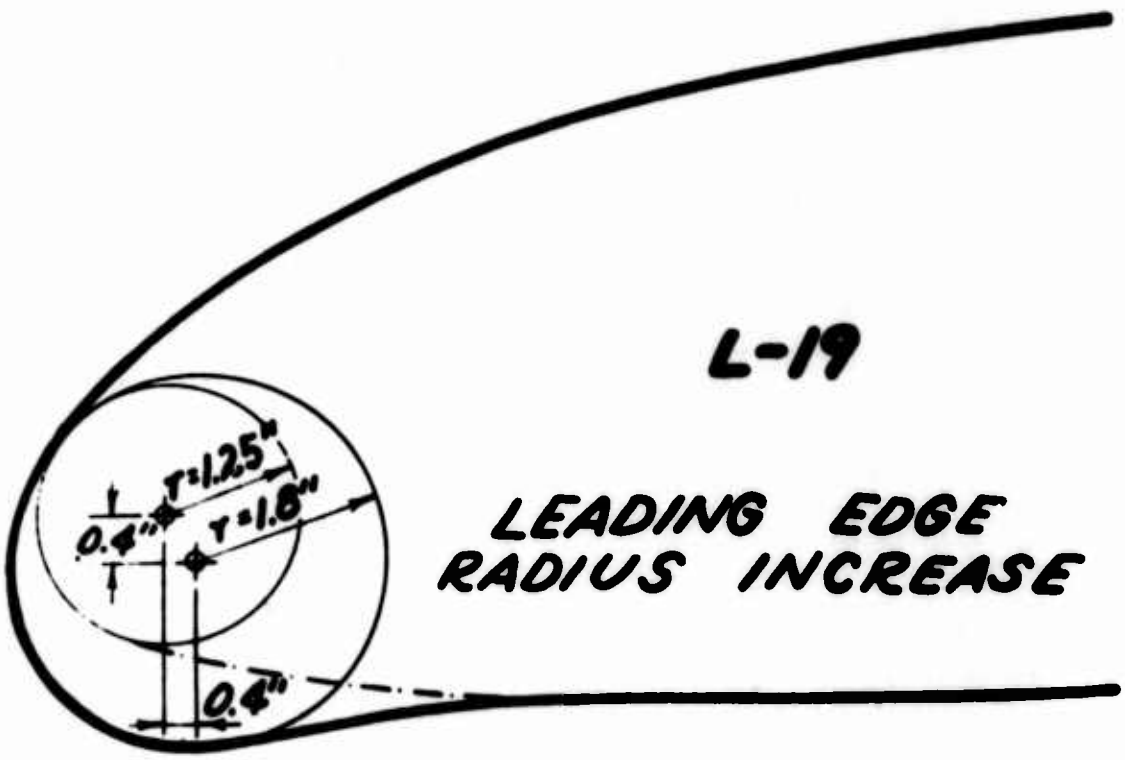

Figure 7. Modification of L-19 Leading Edge.

Standard L-19

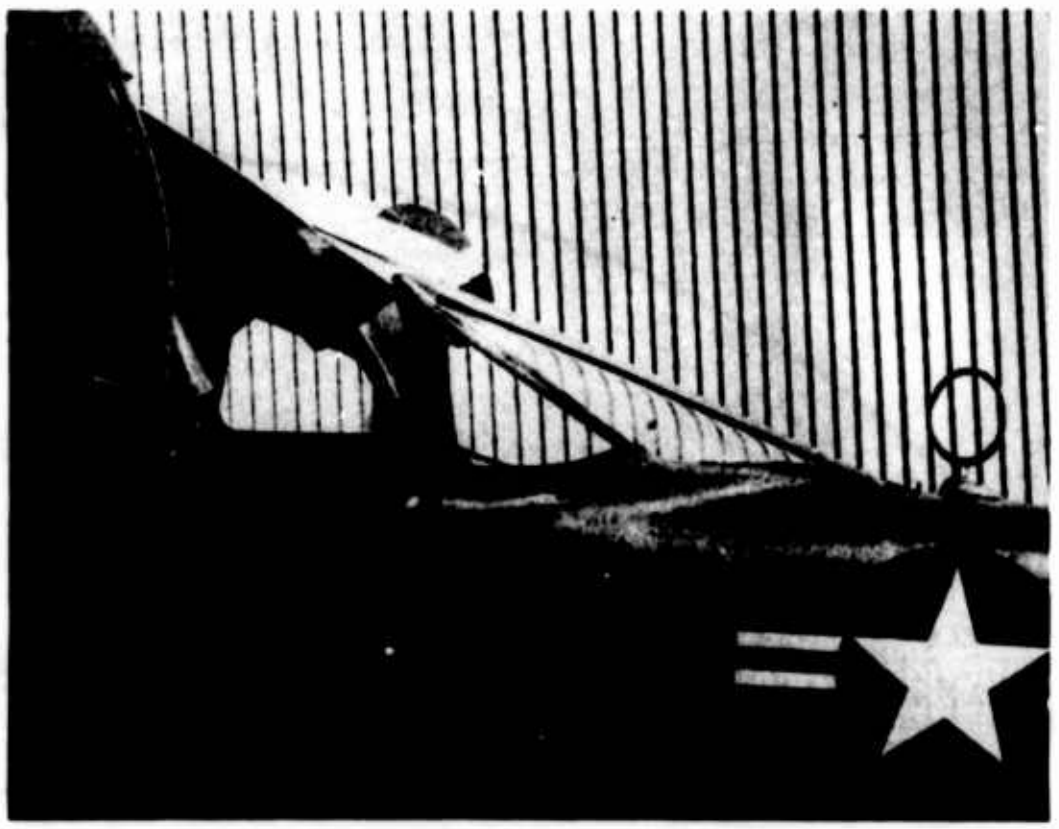

Modified L-19

Figure 8. Modified Aft Canopy of L-19.

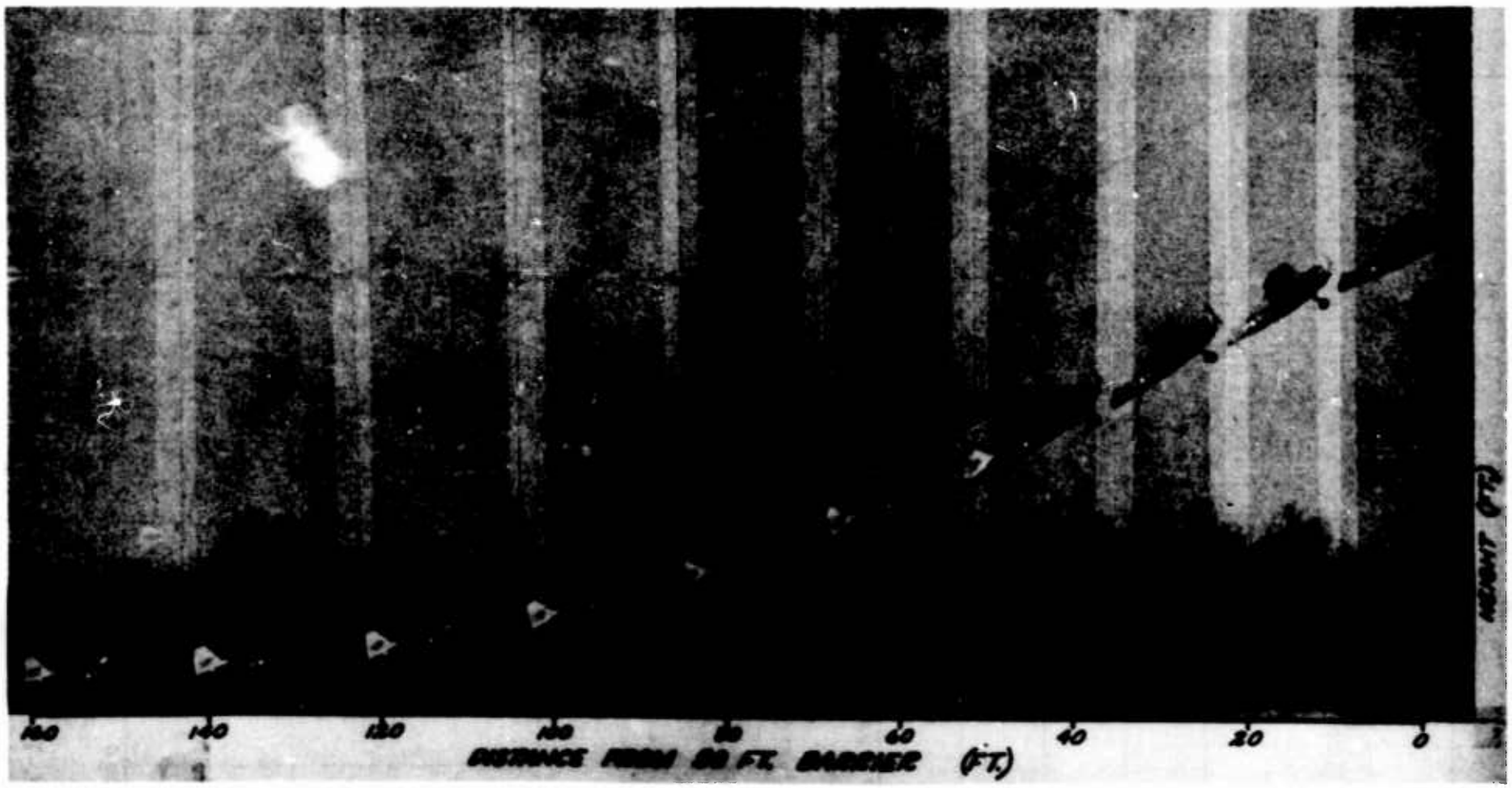

Figure 9. Typical Series of L-19 Take-Off Pictures, Full Flaps, BLC Blowers On.

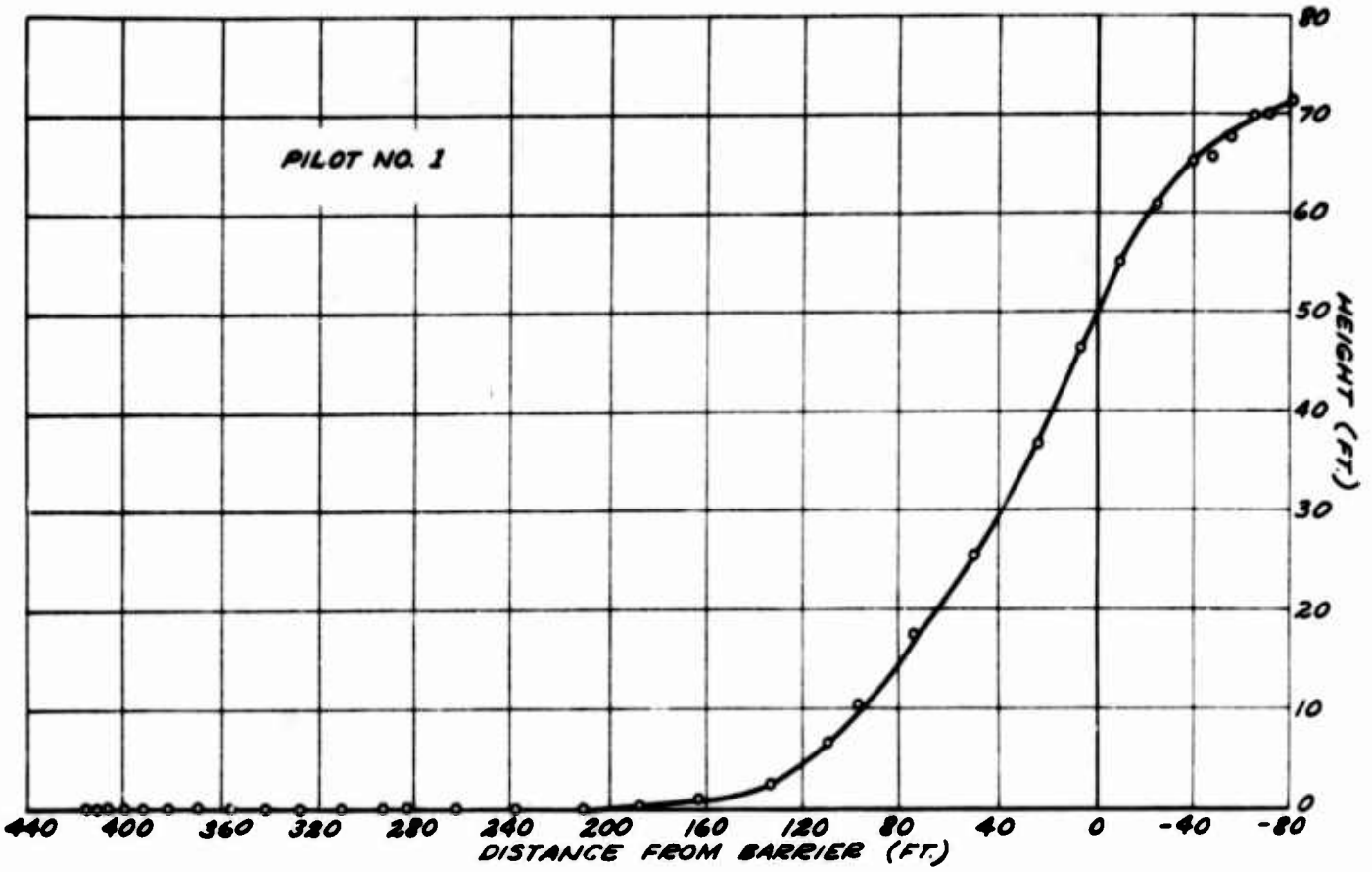

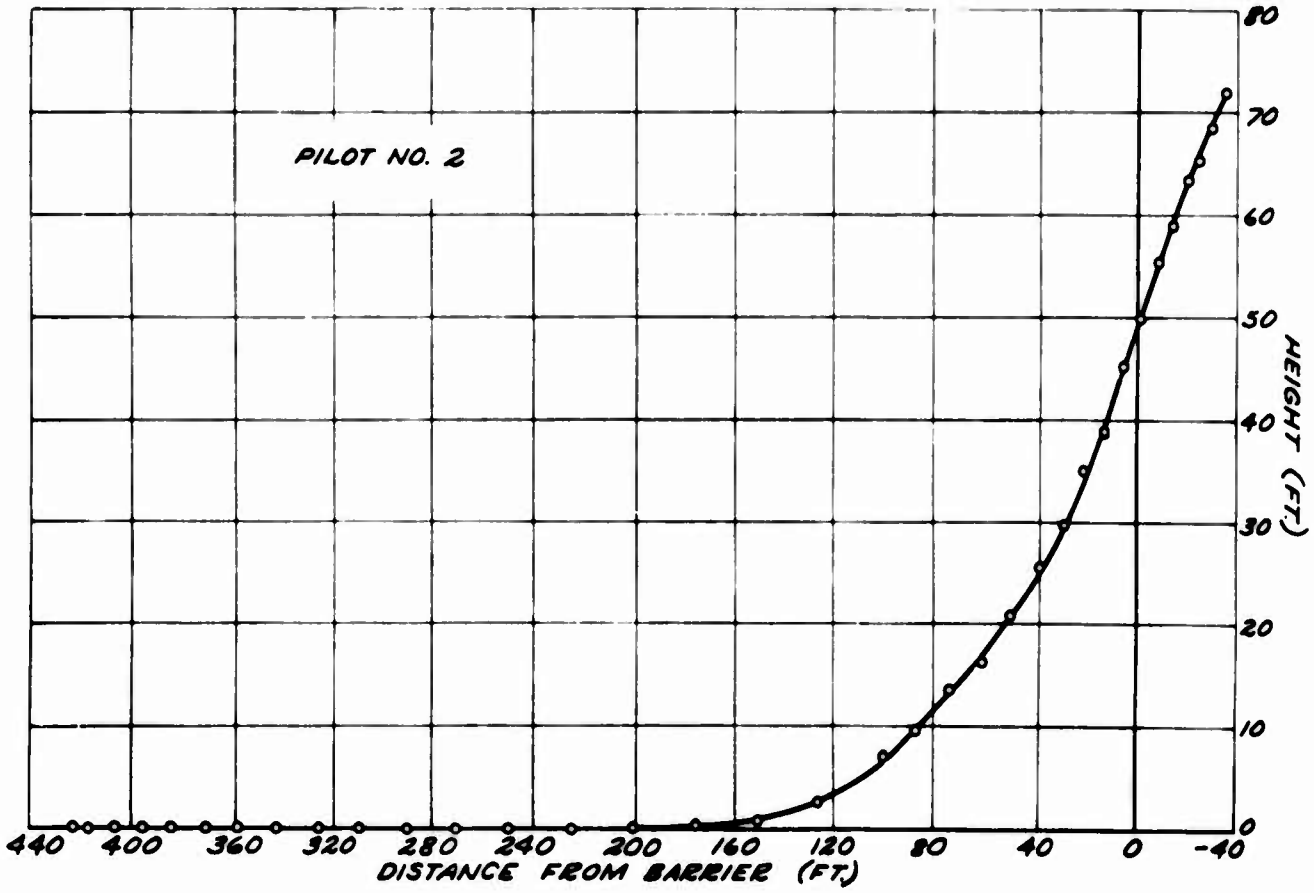

Figure 10. L-19 Take-Off Measurements, Full Flaps, BLC Blowers On, W_s = 2300 Pounds.

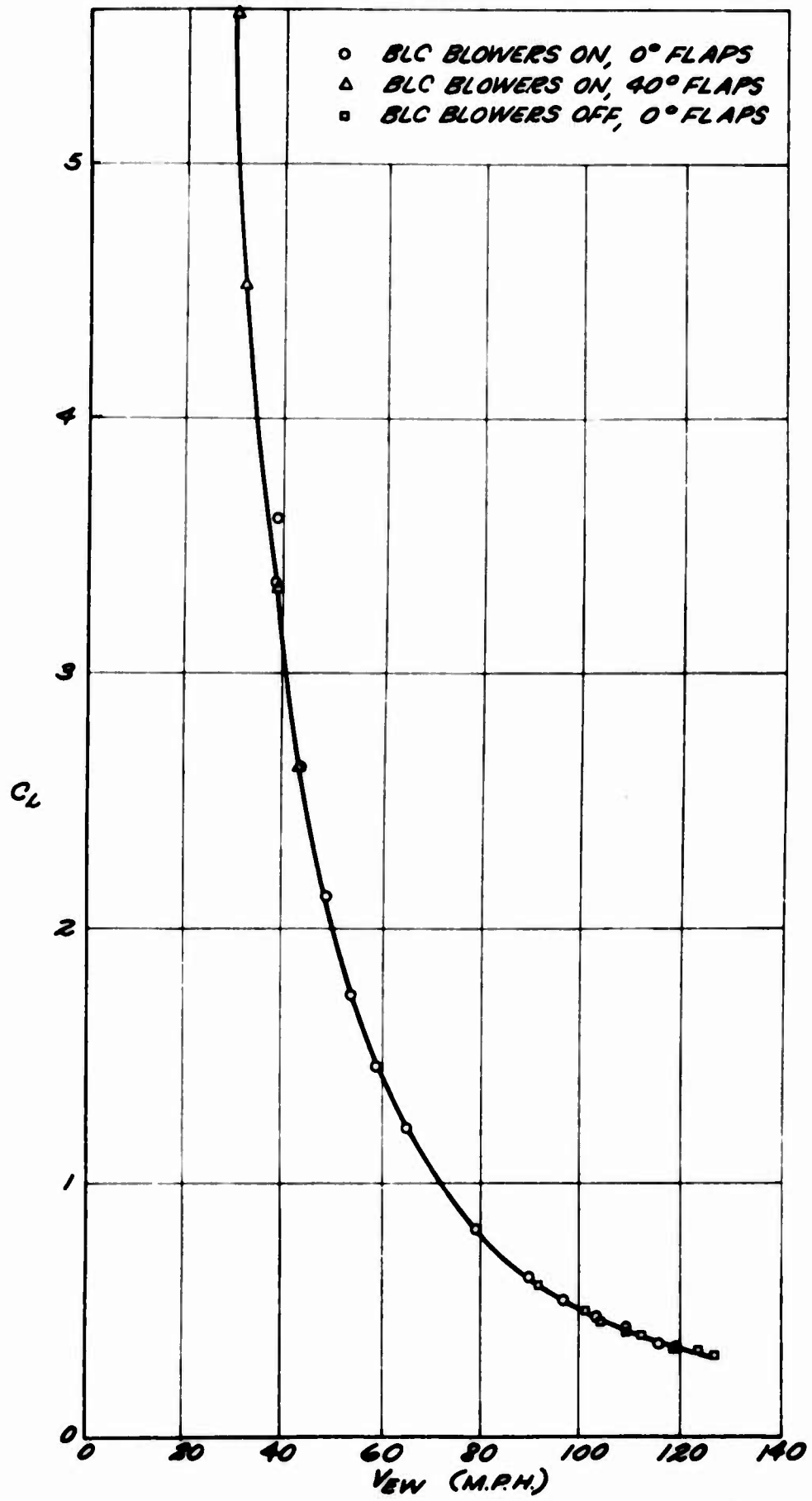

Figure 11. Aircraft Lift Coefficient Against Equivalent Airspeed.

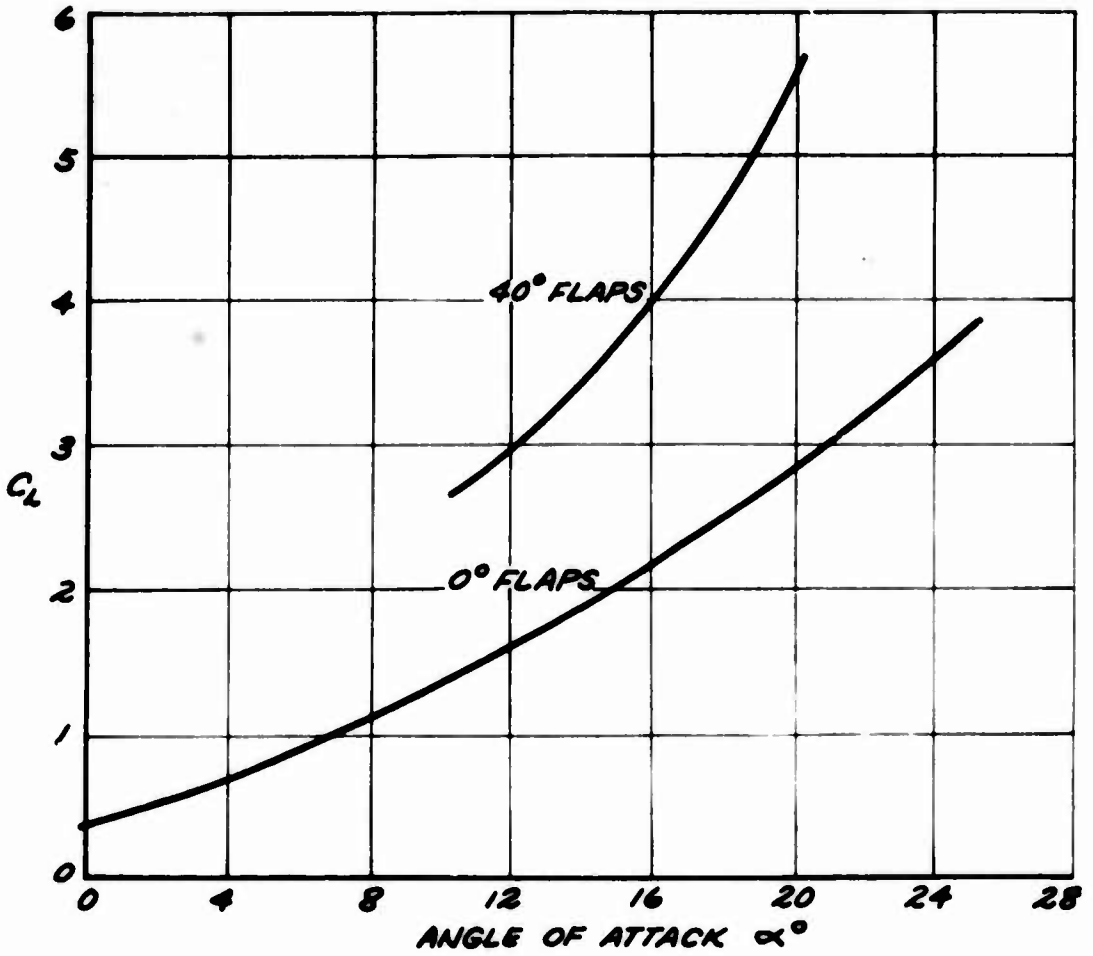

Figure 12. Aircraft Lift Coefficient Against Angle of Attack.

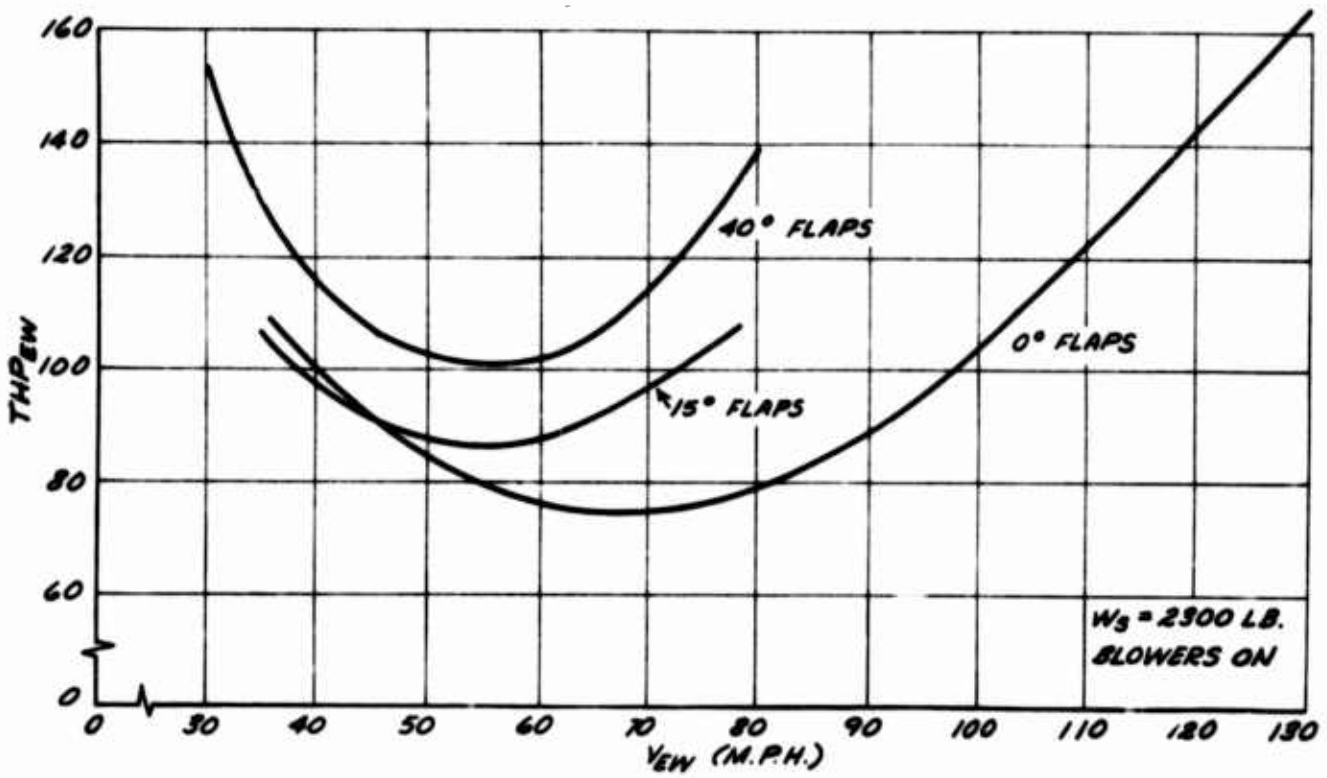

Figure 13. Power Required for Level Flight.

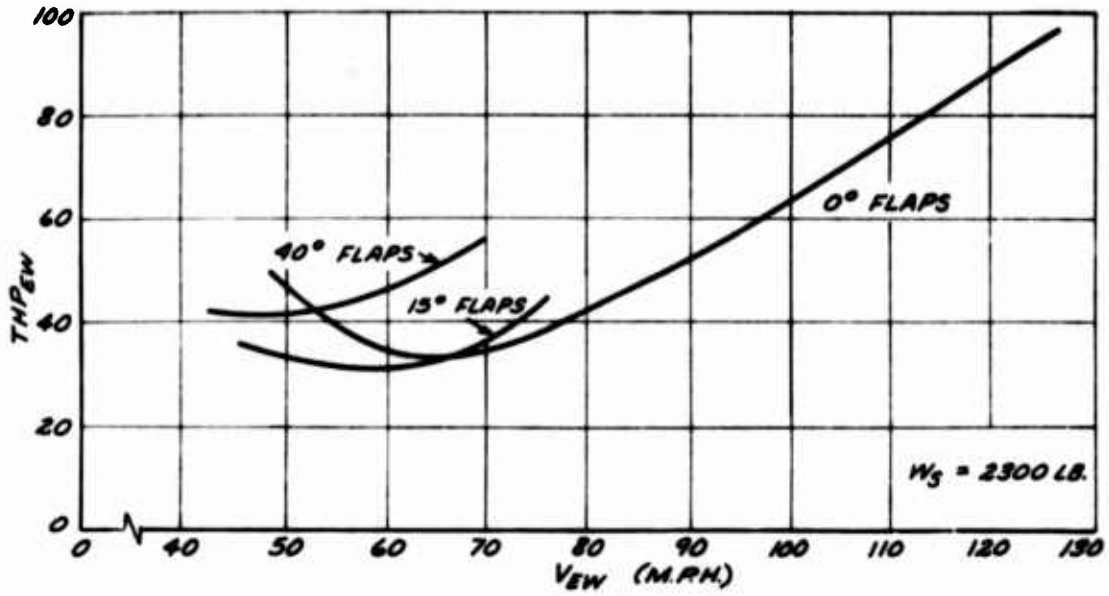

Figure 14. Power Required in Gliding Flight.

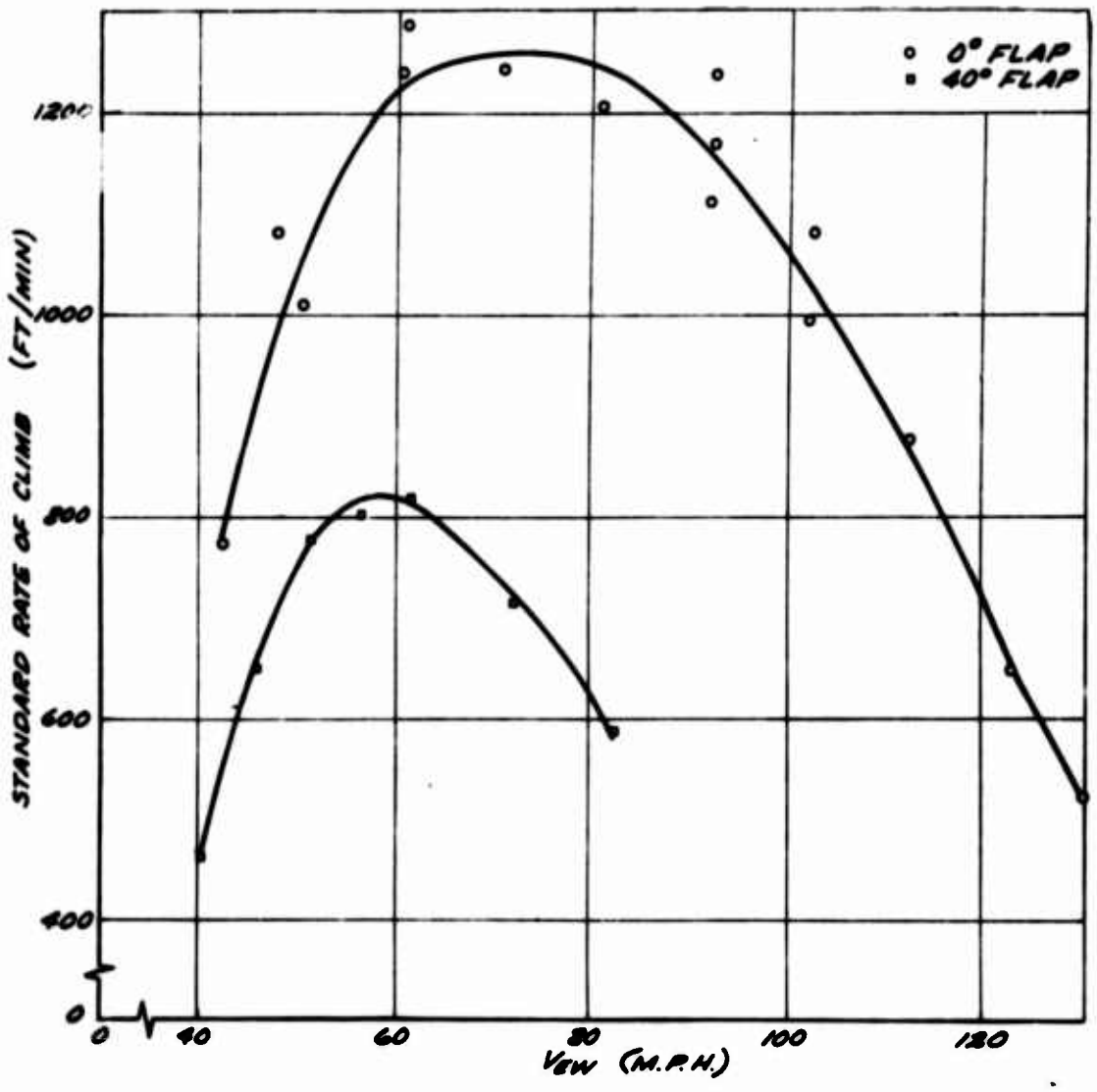

Figure 15. Climb Performance Tests.

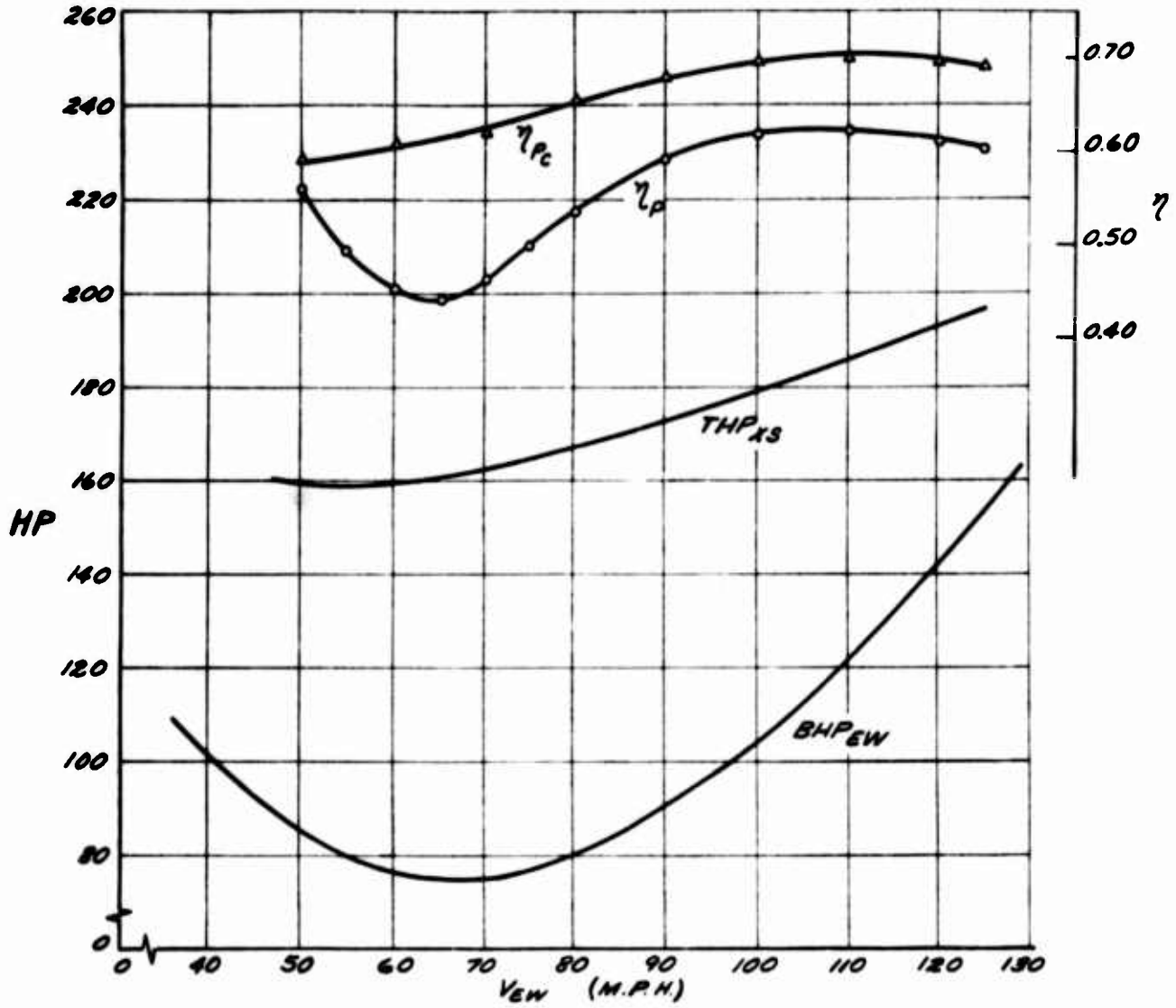

Figure 16. Excess Horsepower Available for Climb and Propulsive Efficiency.

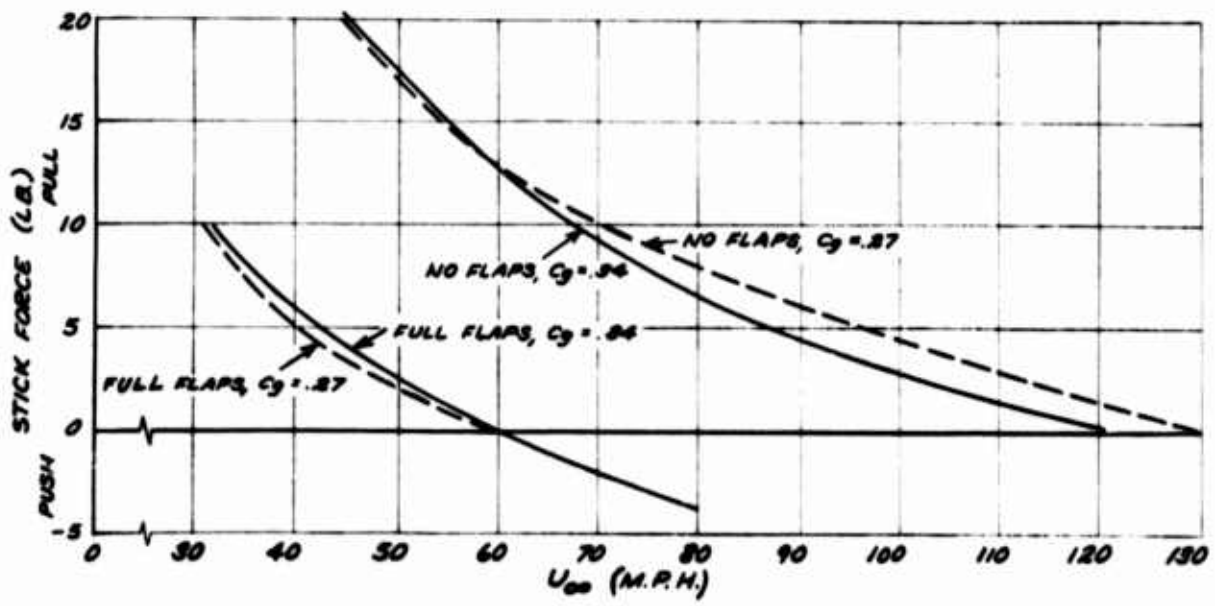

Figure 17. Stick Force Measurements on Modified L-19.

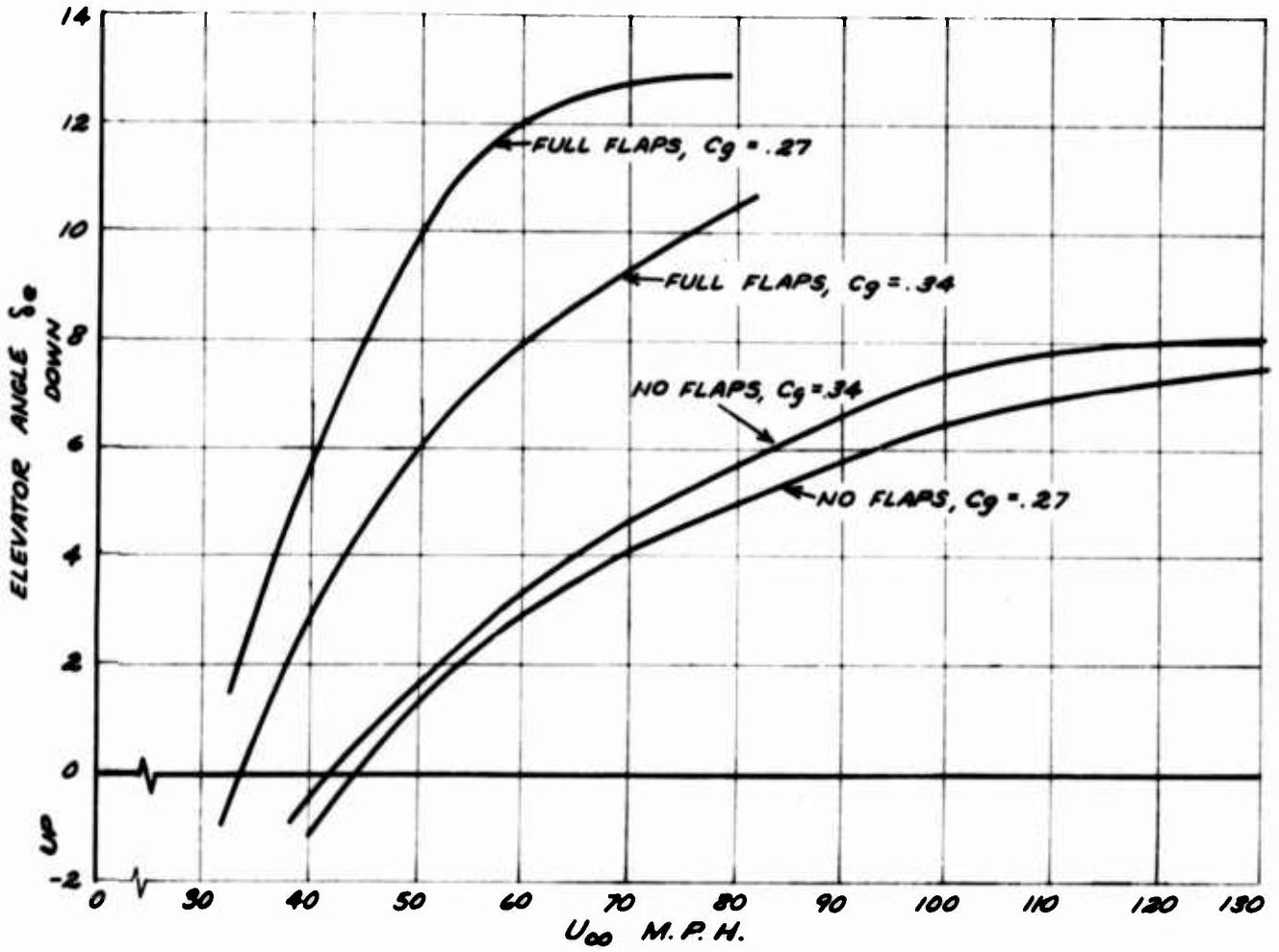

Figure 18. Elevator Angle Measurements on Modified L-19.

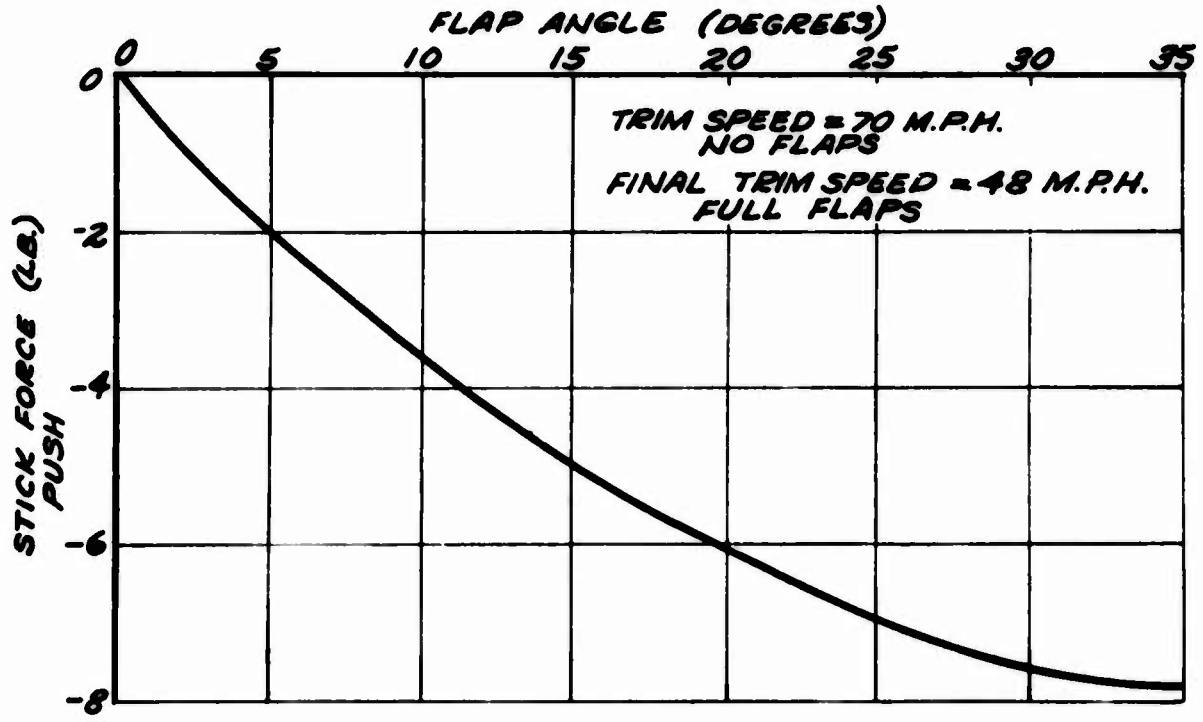

Figure 19. Stick Force as a Function of Flap Angle, Constant Power.

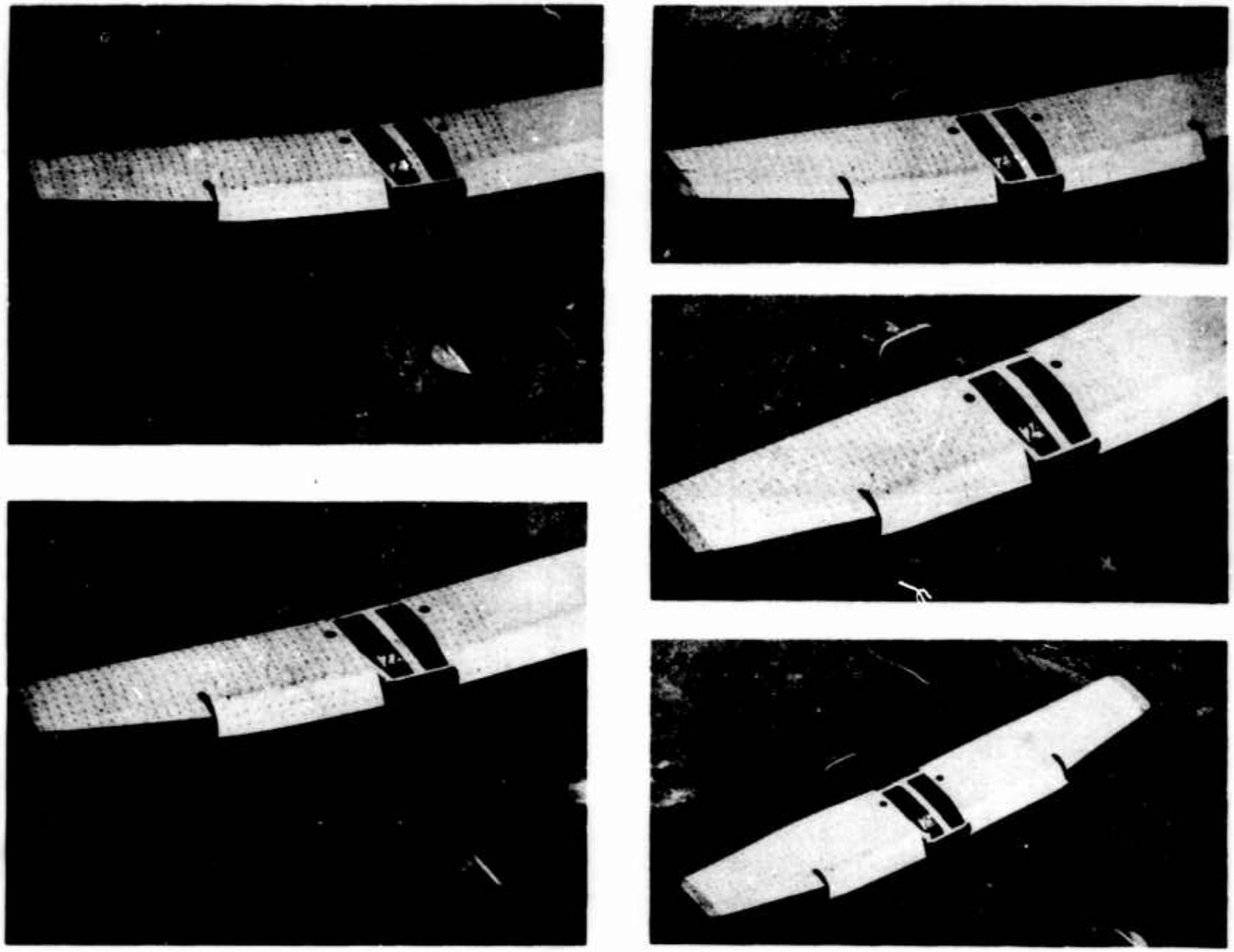

Figure 20. Wing Stall Patterns, Full Flaps, BLC Blowers On.

Figure 21. Manometer Arrangement in Rear Cockpit of L-19.

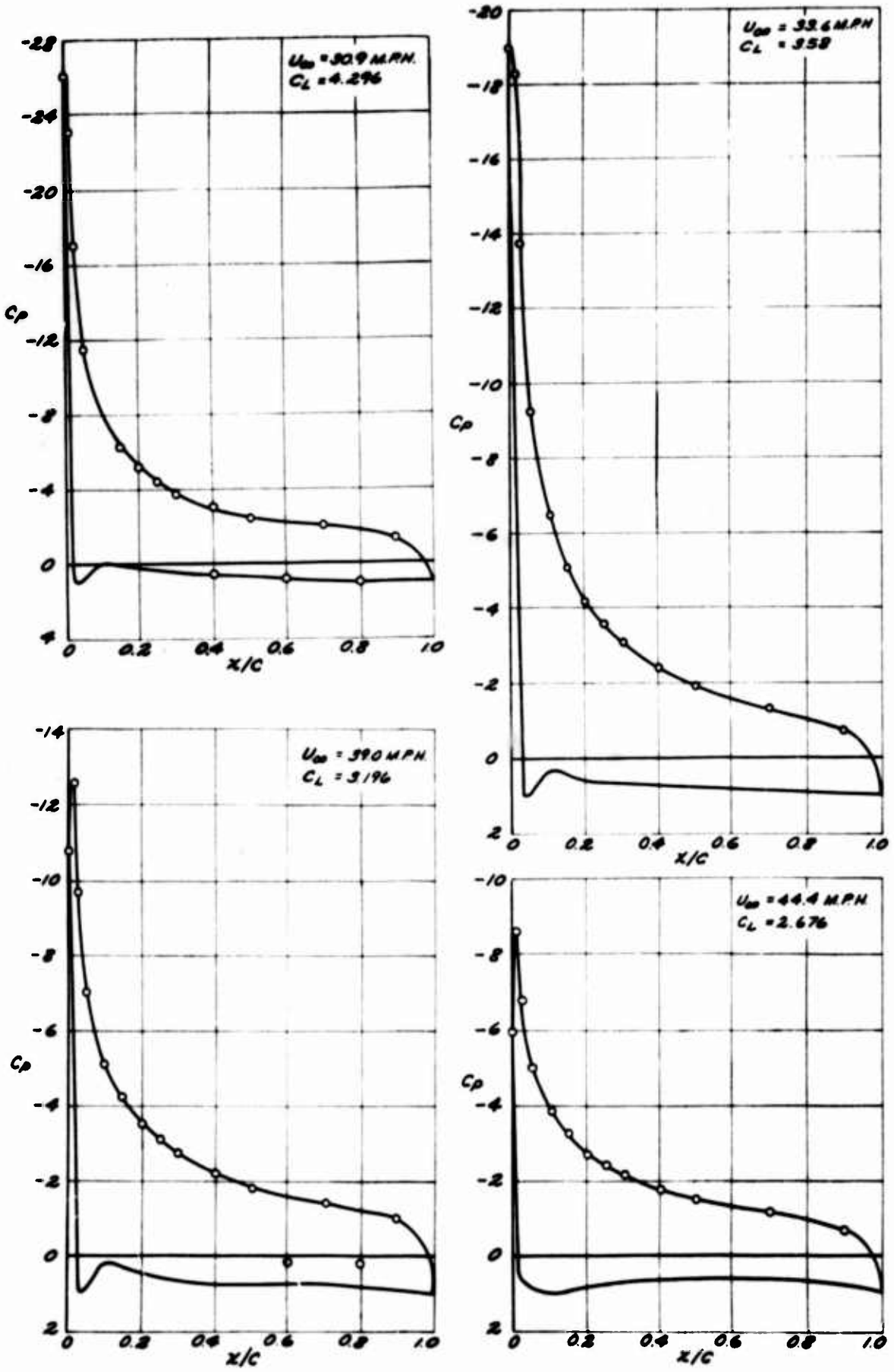

Figure 22. Wing Pressure Distributions at Various Aircraft Airspeeds, Full Flaps, BLC Blowers On.

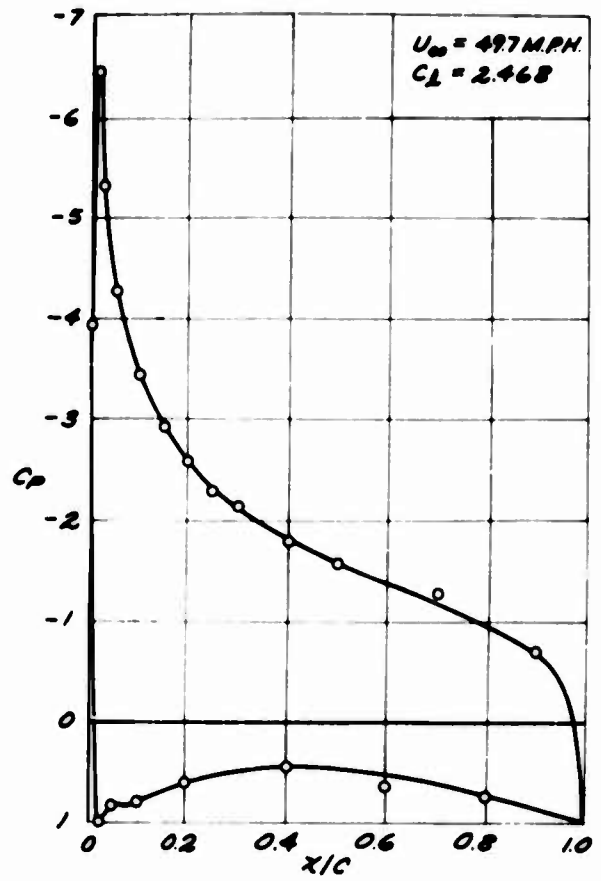

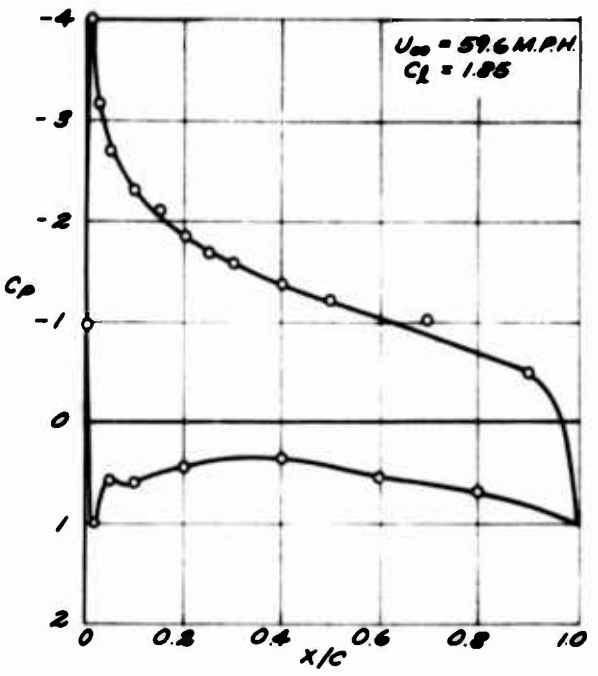

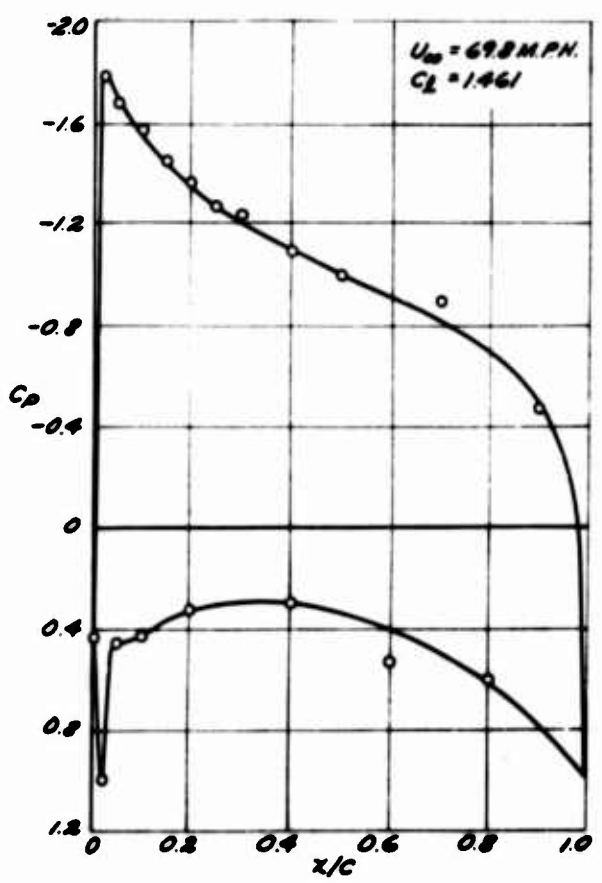

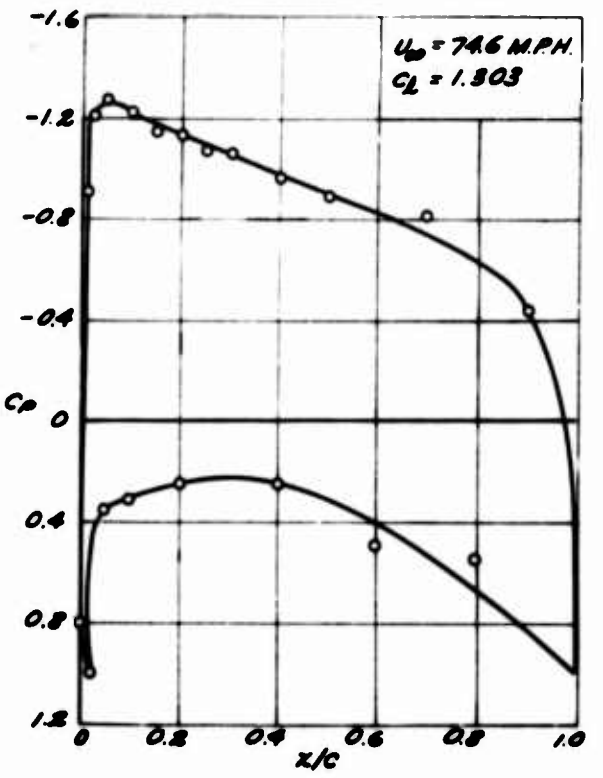

Figure 22 (Cont.). Wing Pressure Distributions at Various Aircraft Airspeeds, Full Flaps, BLC Blowers On.

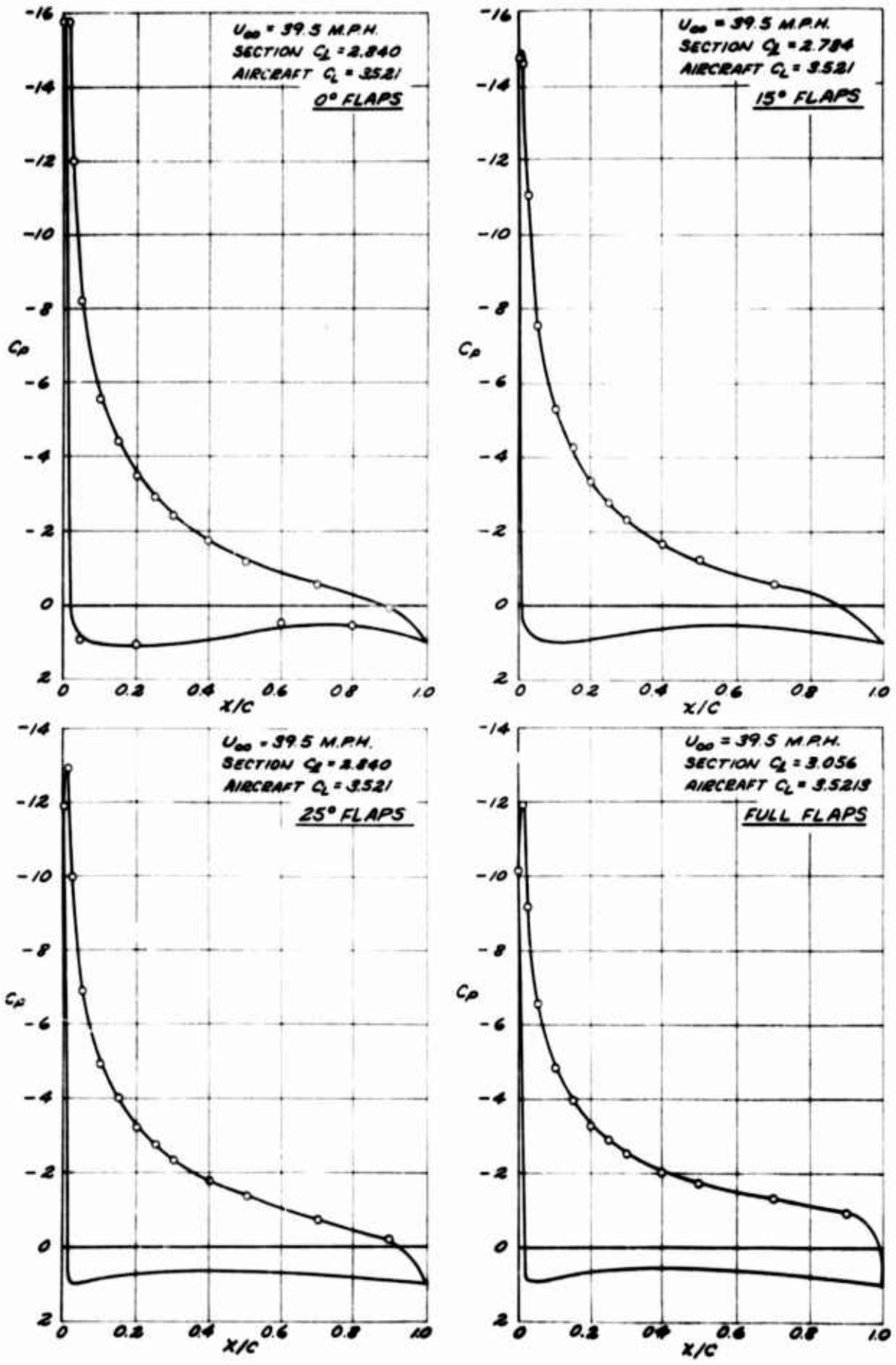

Figure 23. Effect of Flap Angle on Pressure Distribution at a Constant Aircraft Airspeed, BLC Blowers On.

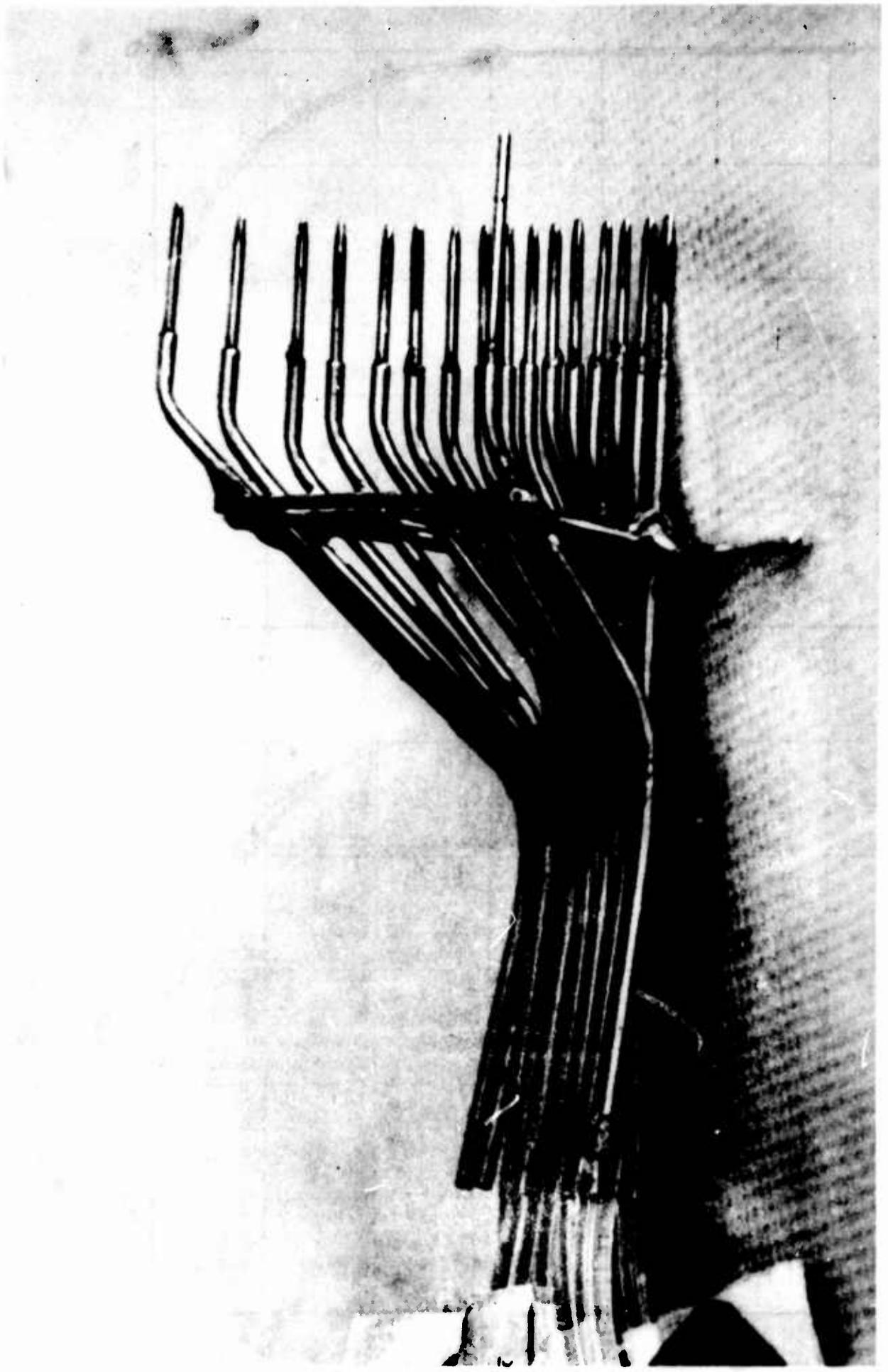

Figure 24. Boundary Layer Probe.

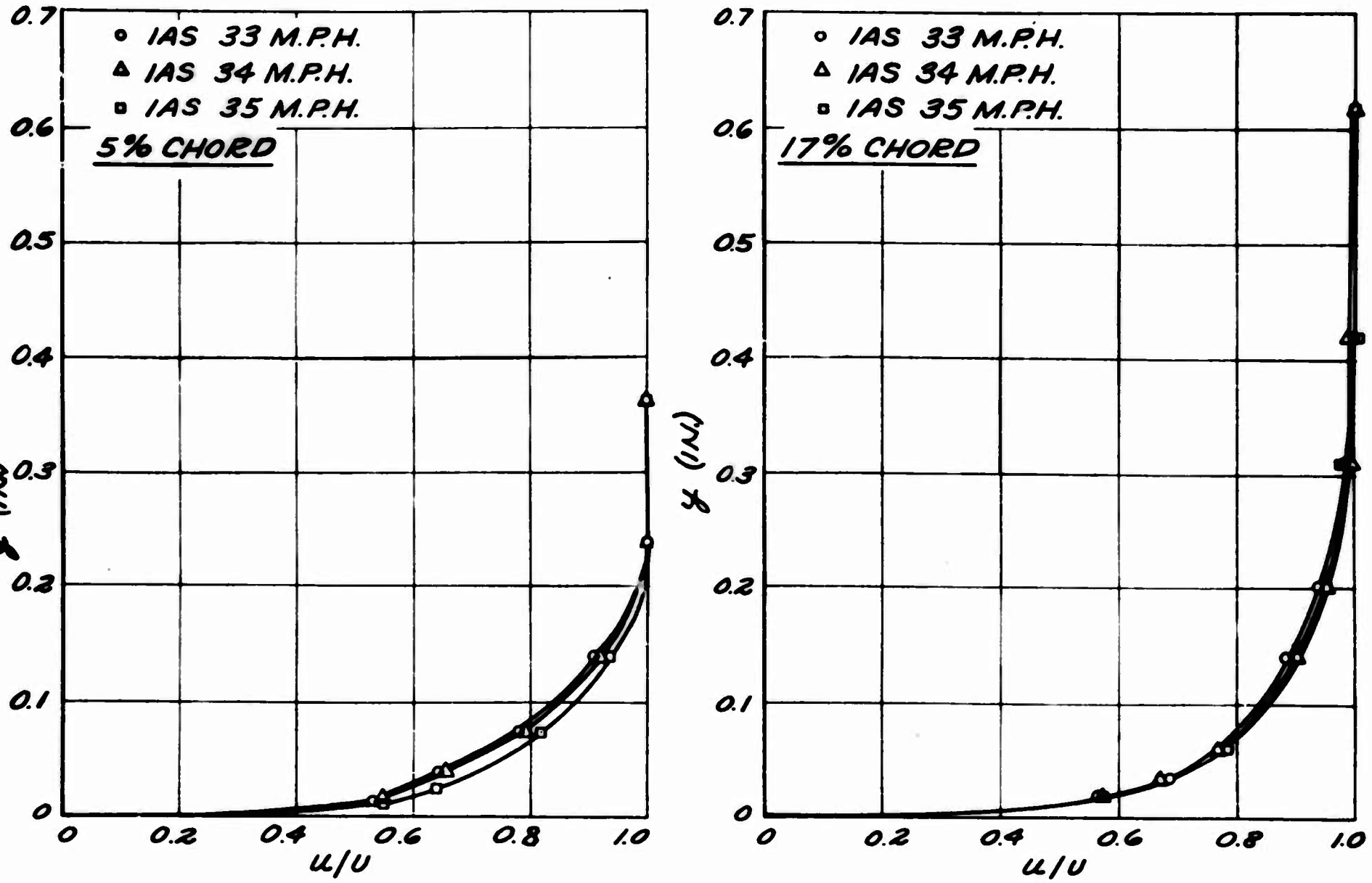

Figure 25. Typical Series of Boundary Layer Profiles, Full Flaps.

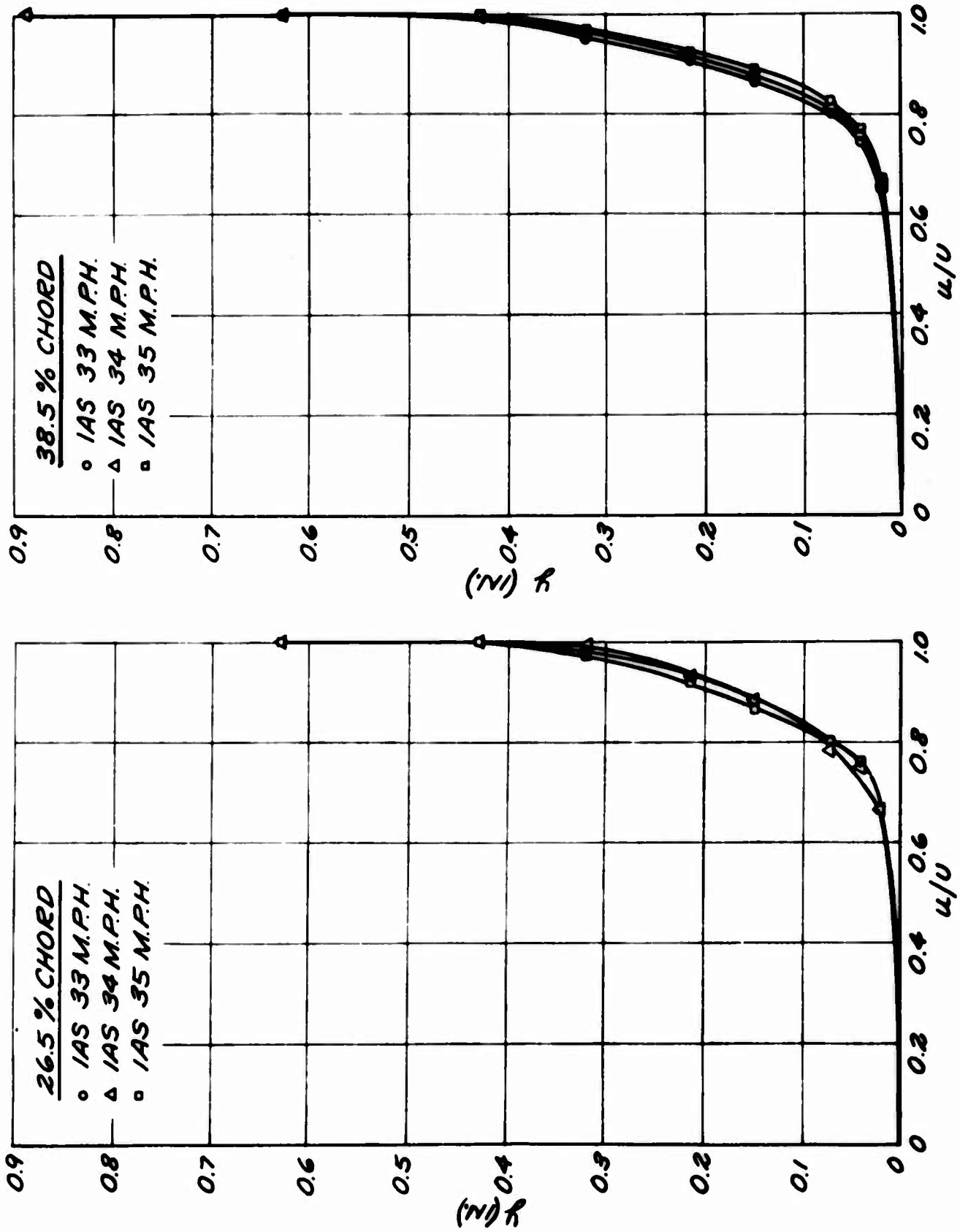

Figure 25 (Cont.). Typical Series of Boundary Layer Profiles, Full Flaps.

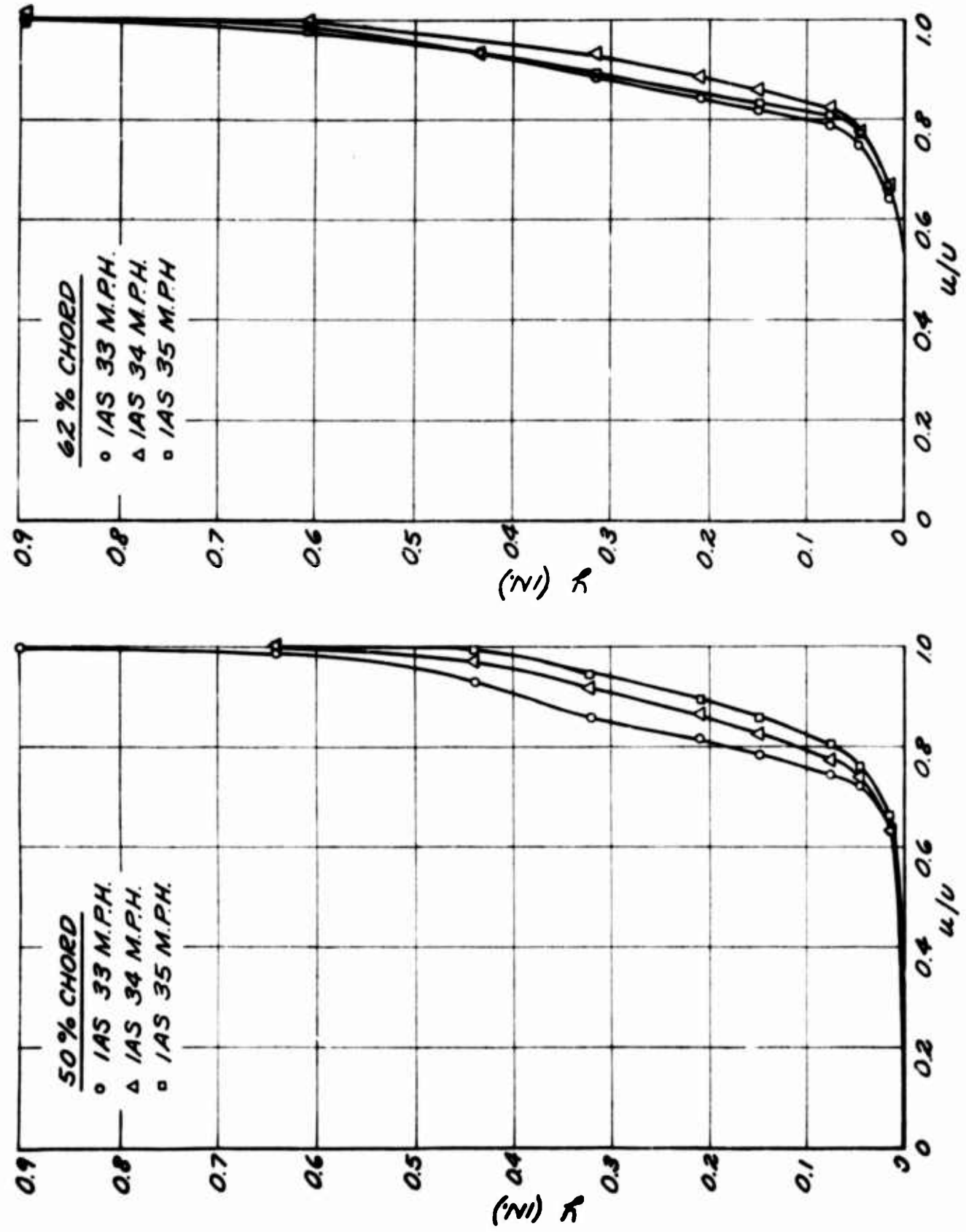

Figure 25 (Cont.). Typical Series of Boundary Layer Profiles, Full Flaps.

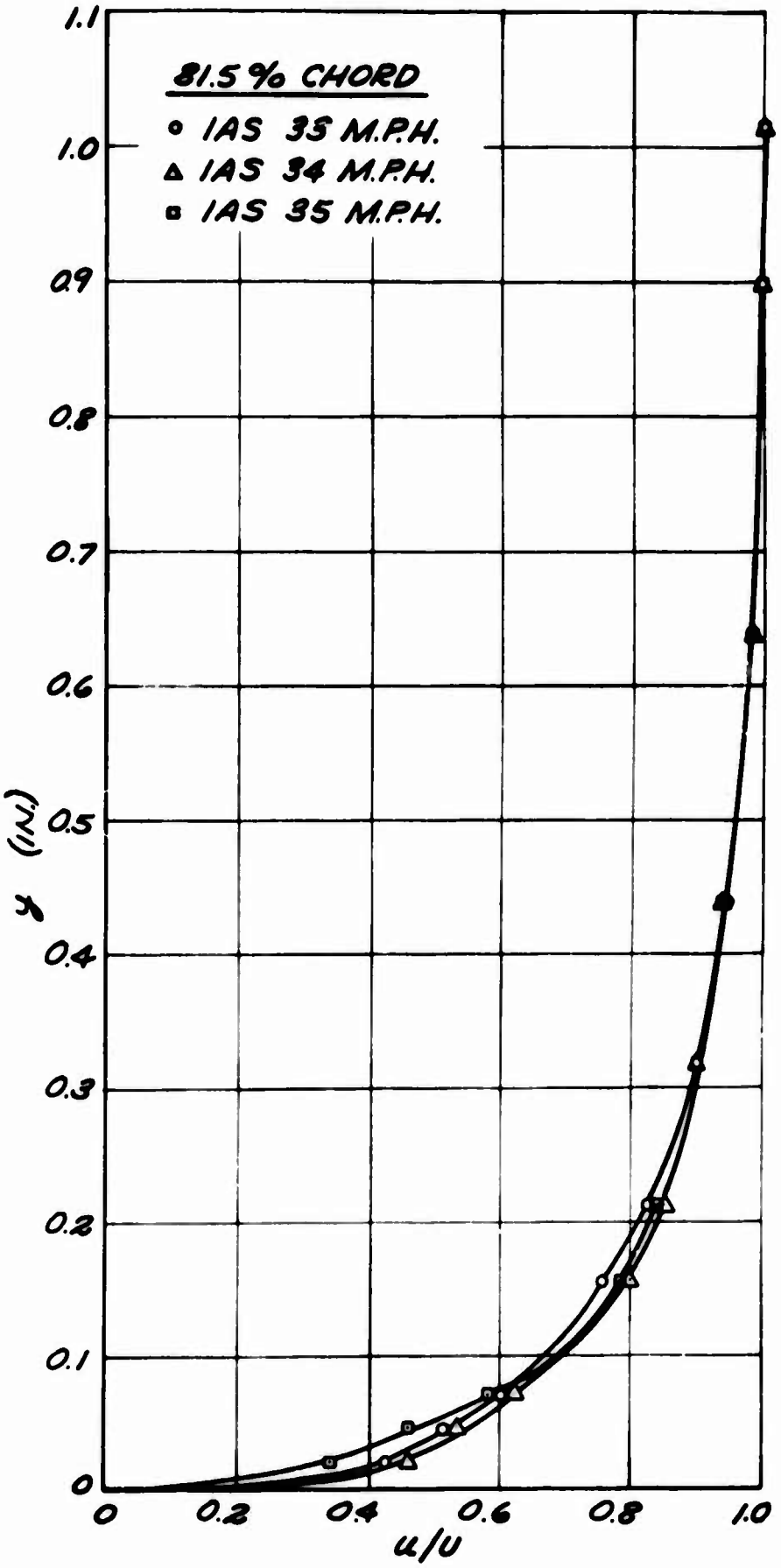

Figure 25 (Cont.). Typical Series of Boundary Layer Profiles, Full Flaps.

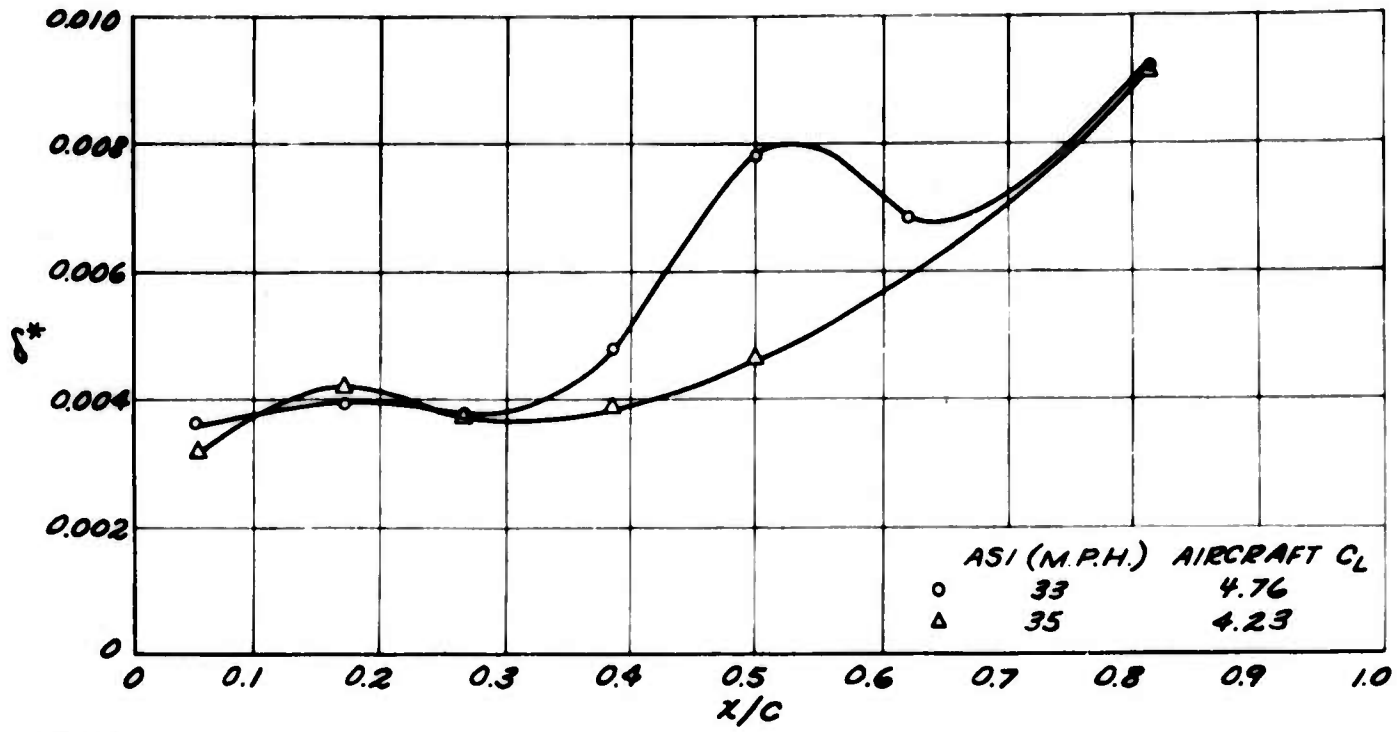

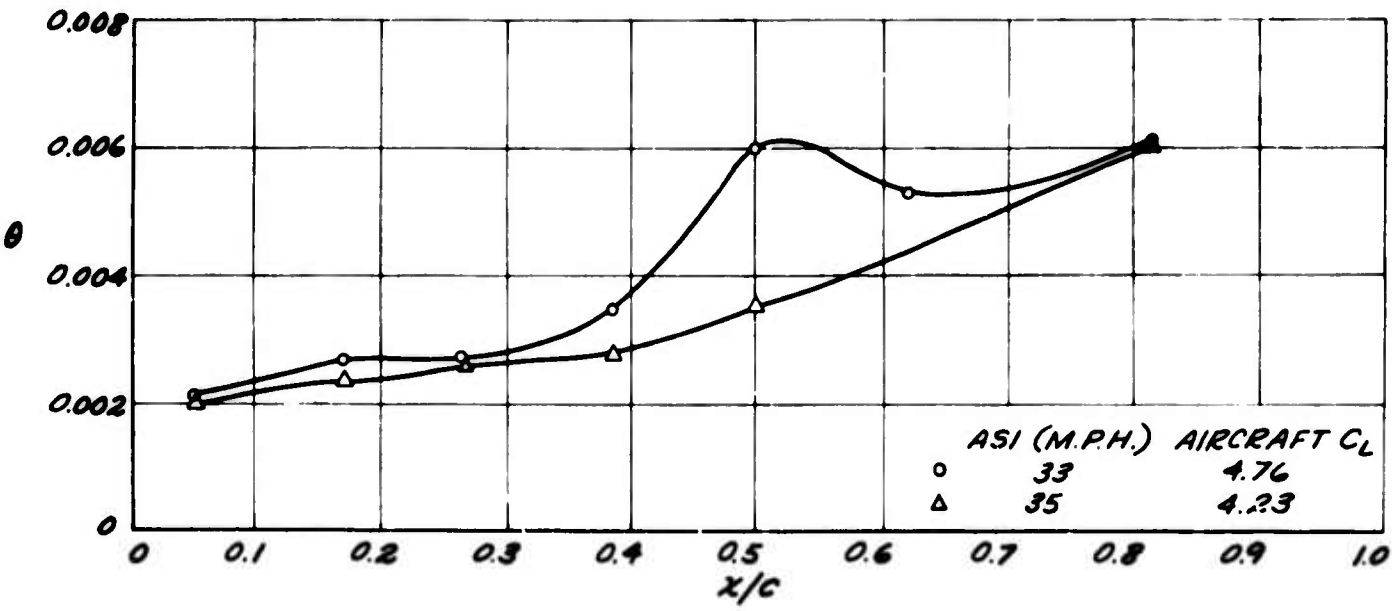

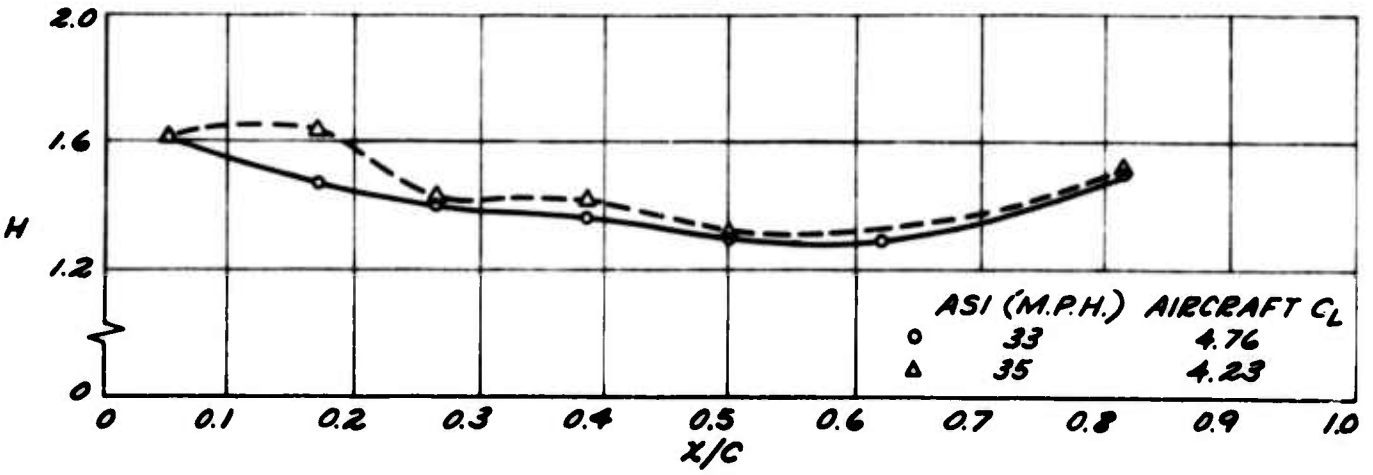

Figure 26. Boundary Layer Parameters (Full Flaps).

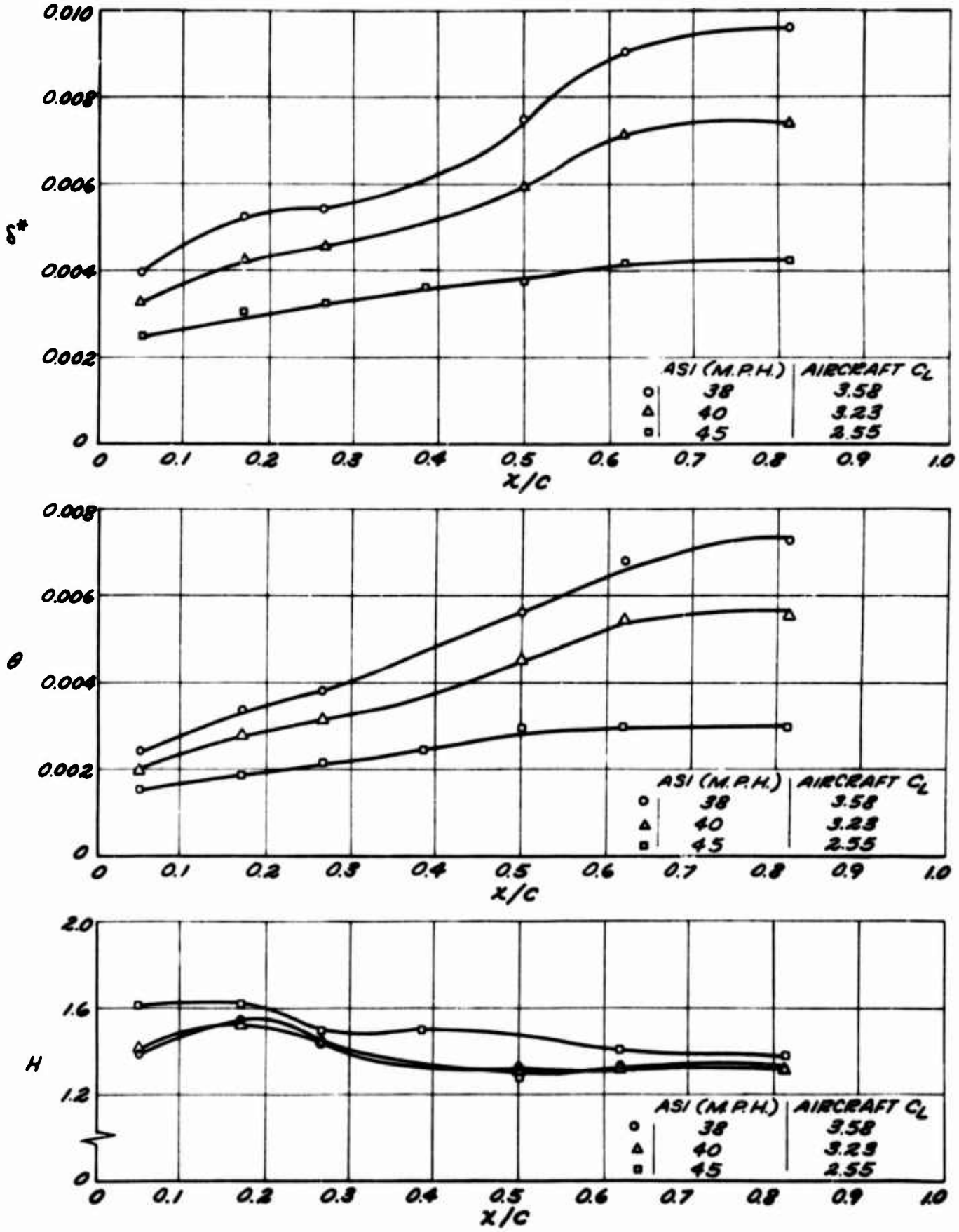

Figure 27. Boundary Layer Parameters (No Flaps).

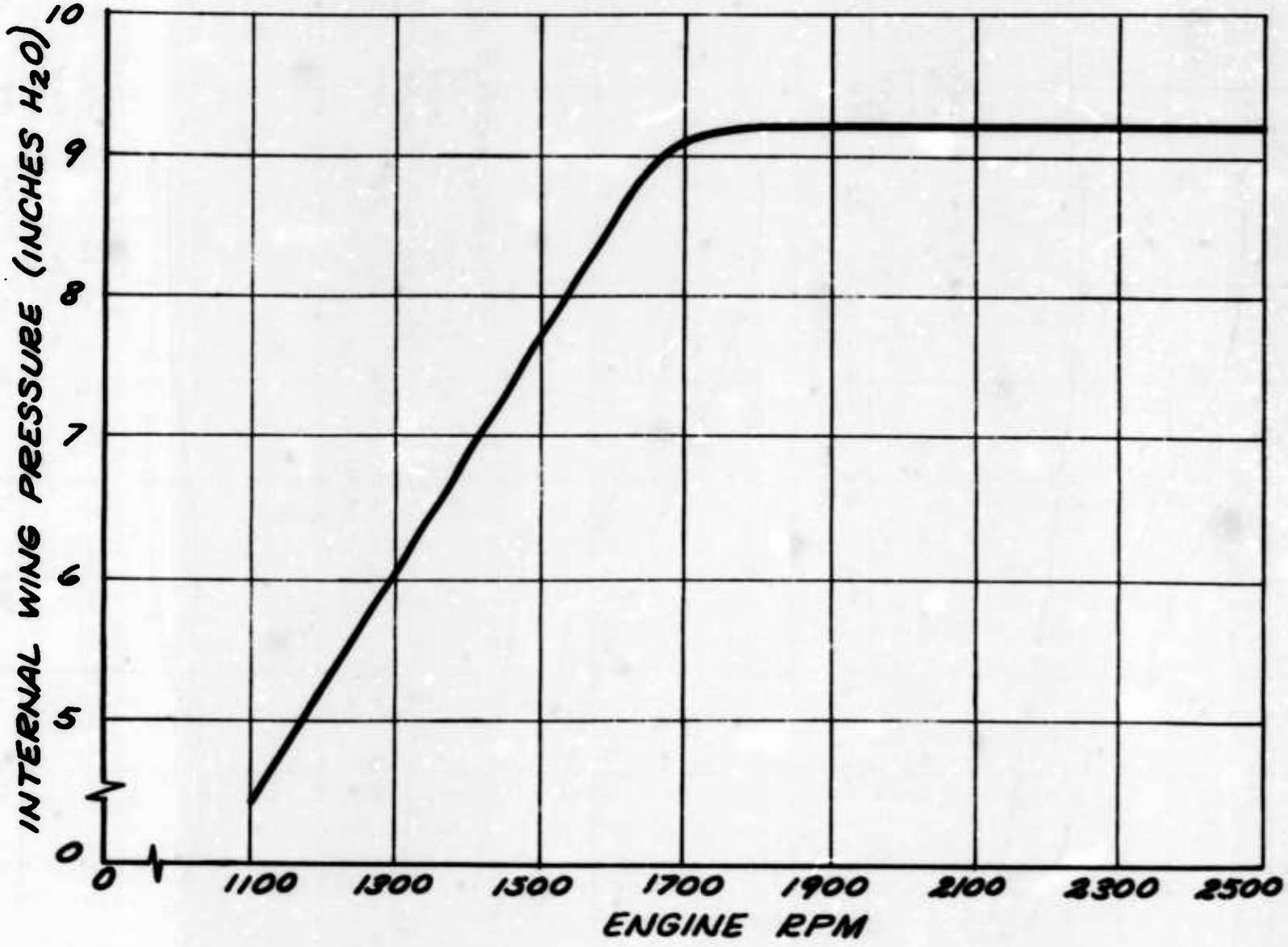

Figure 28. Variation of Wing Internal Pressure With Engine R.P.M.

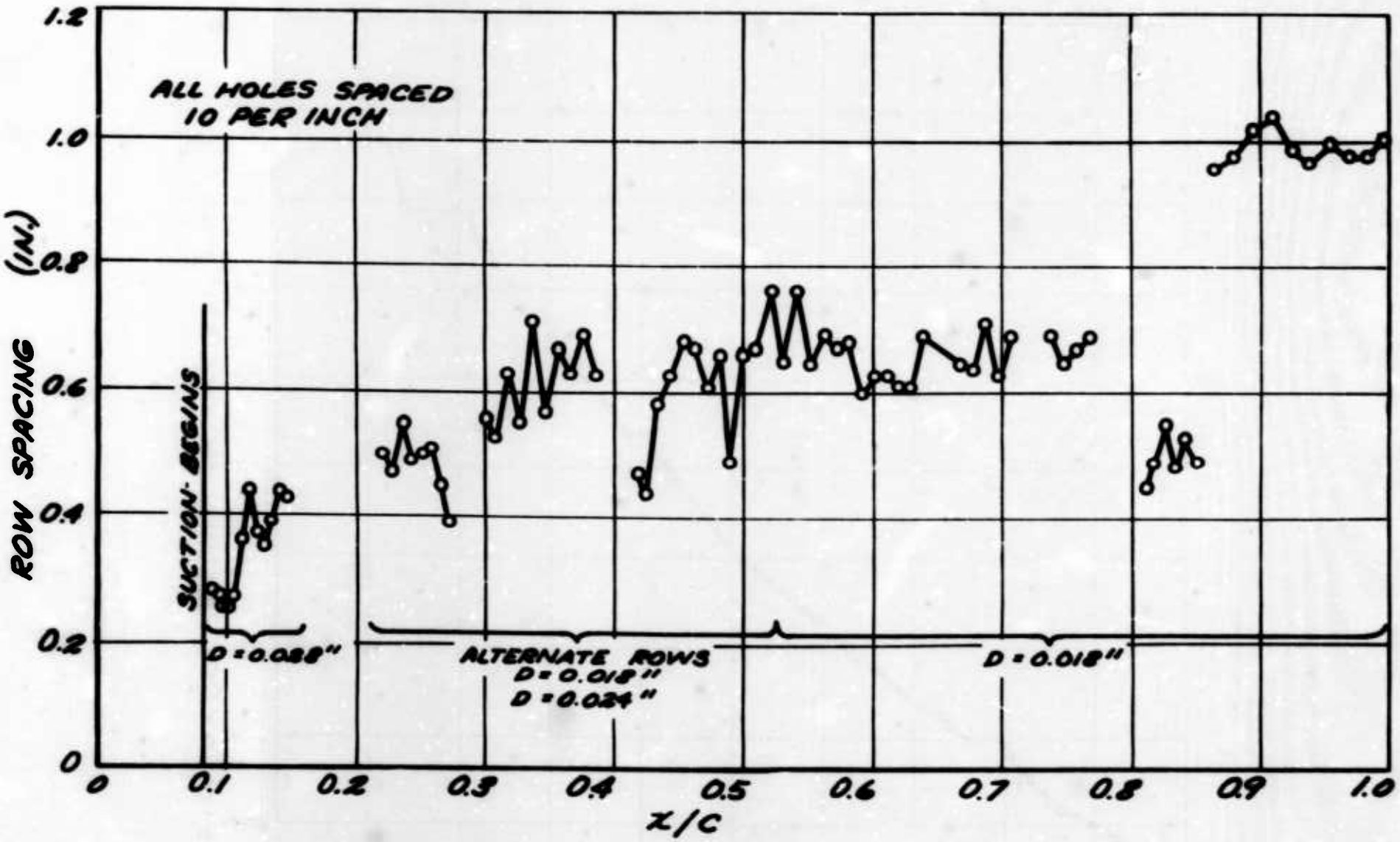

Figure 29. Porosity Distribution Over Flapped Section of L-19 Wing.

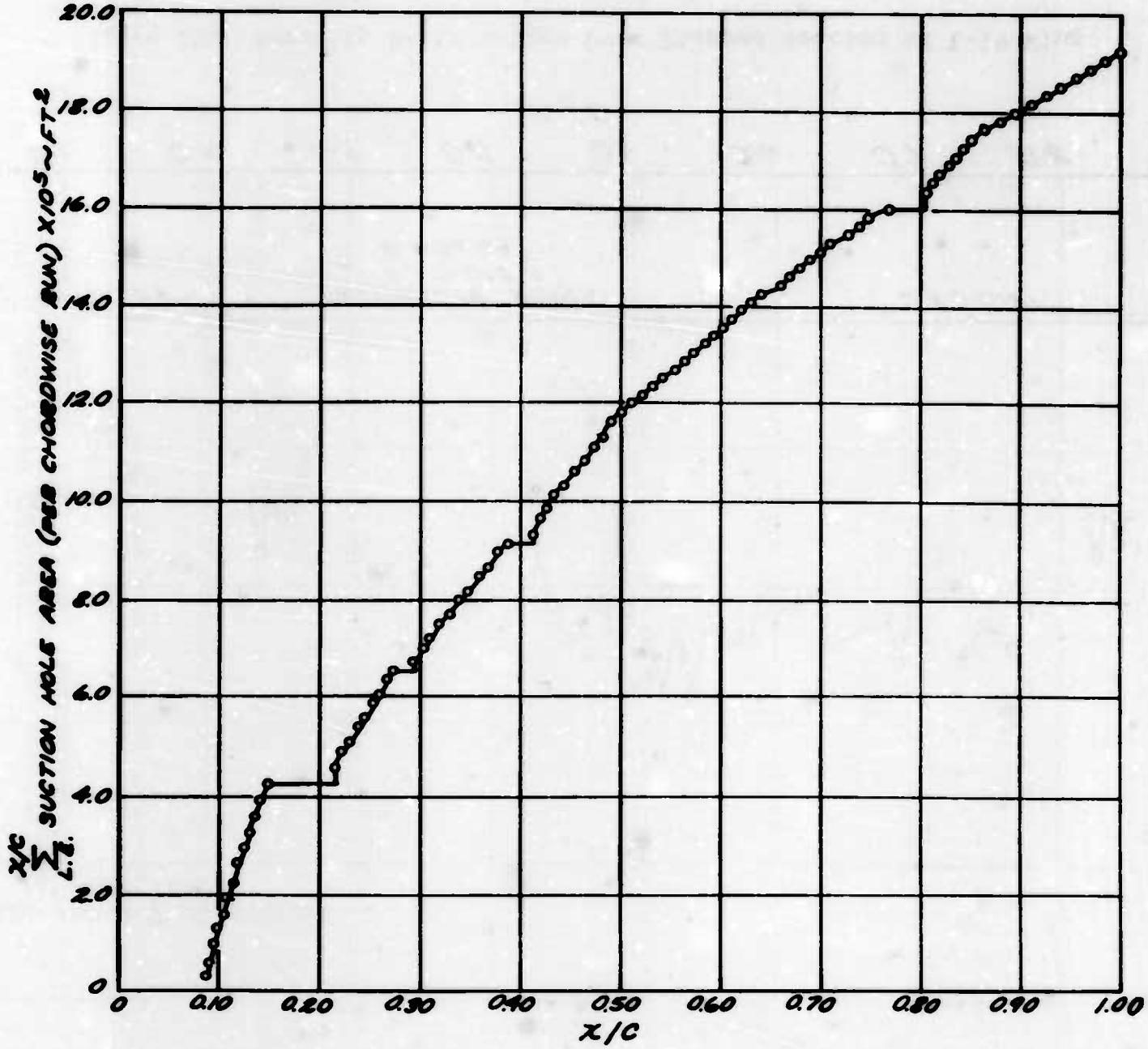

Figure 30. Cumulative Suction Hole Area of L-19 Wing.

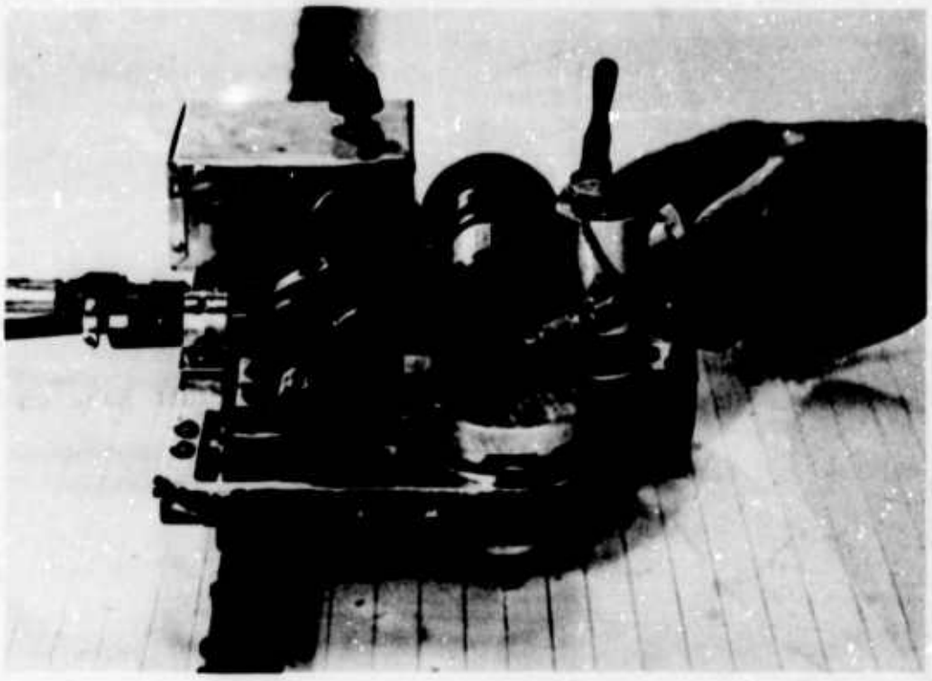

Figure 31. Photograph of Pneumatic Drilling Machine.

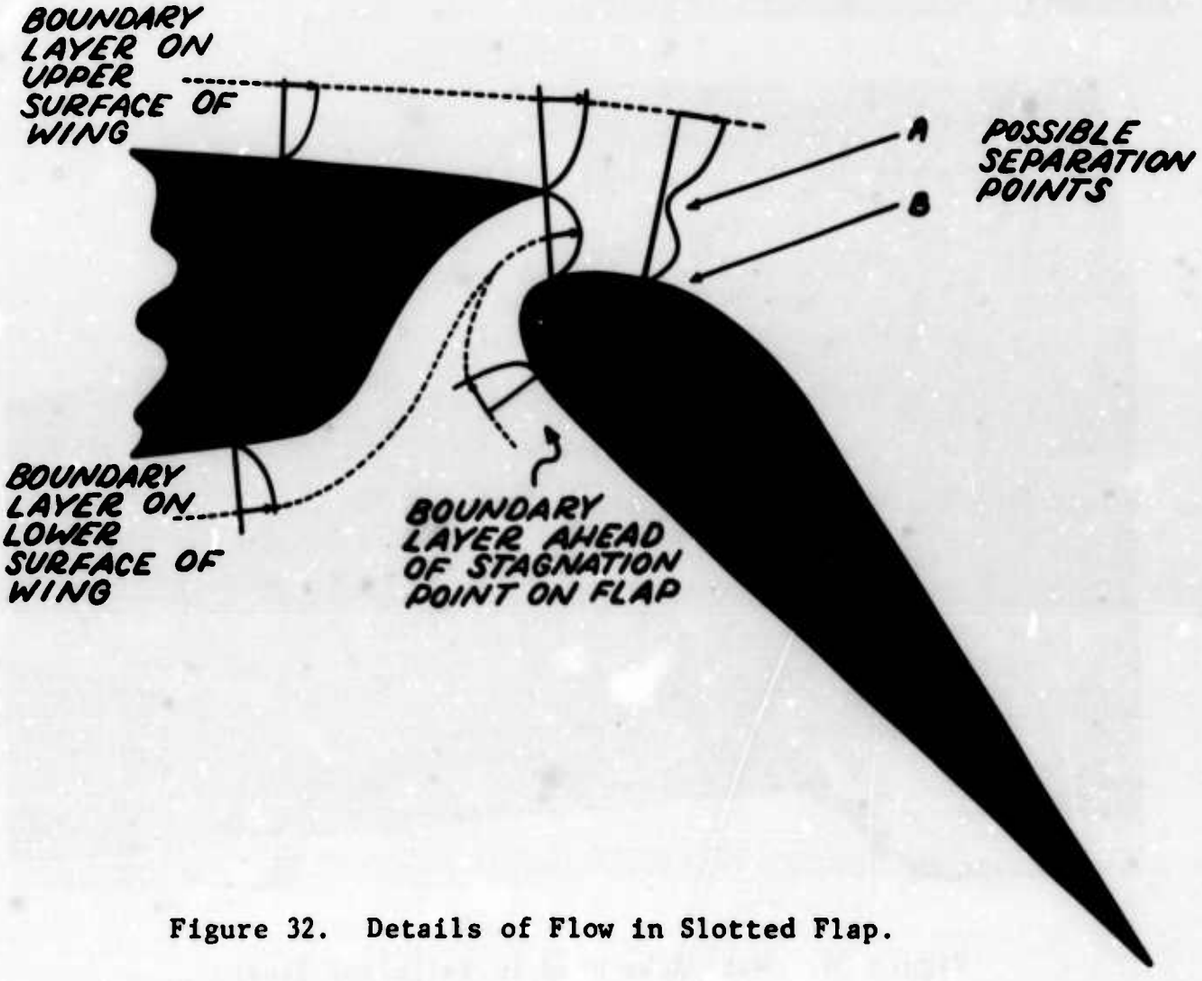

Figure 32. Details of Flow in Slotted Flap.

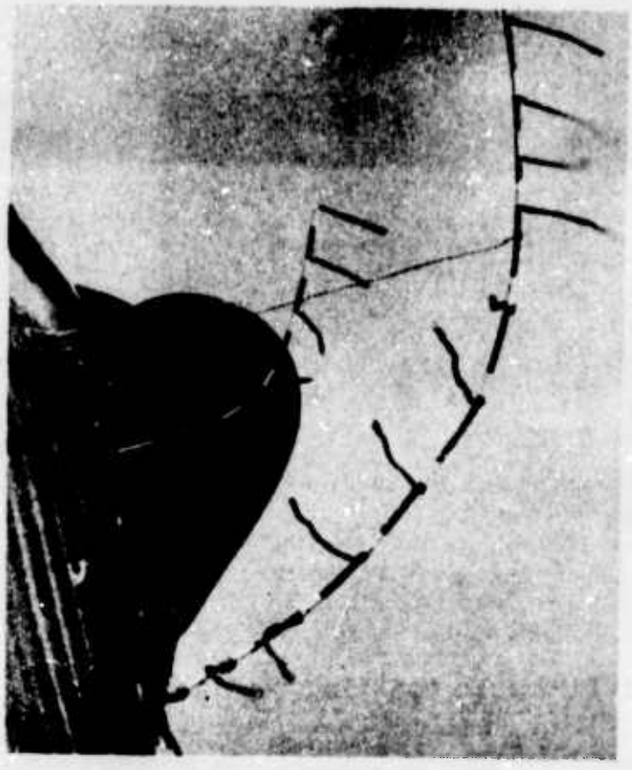

Figure 33. Tuft Rake on L-19 Flap.

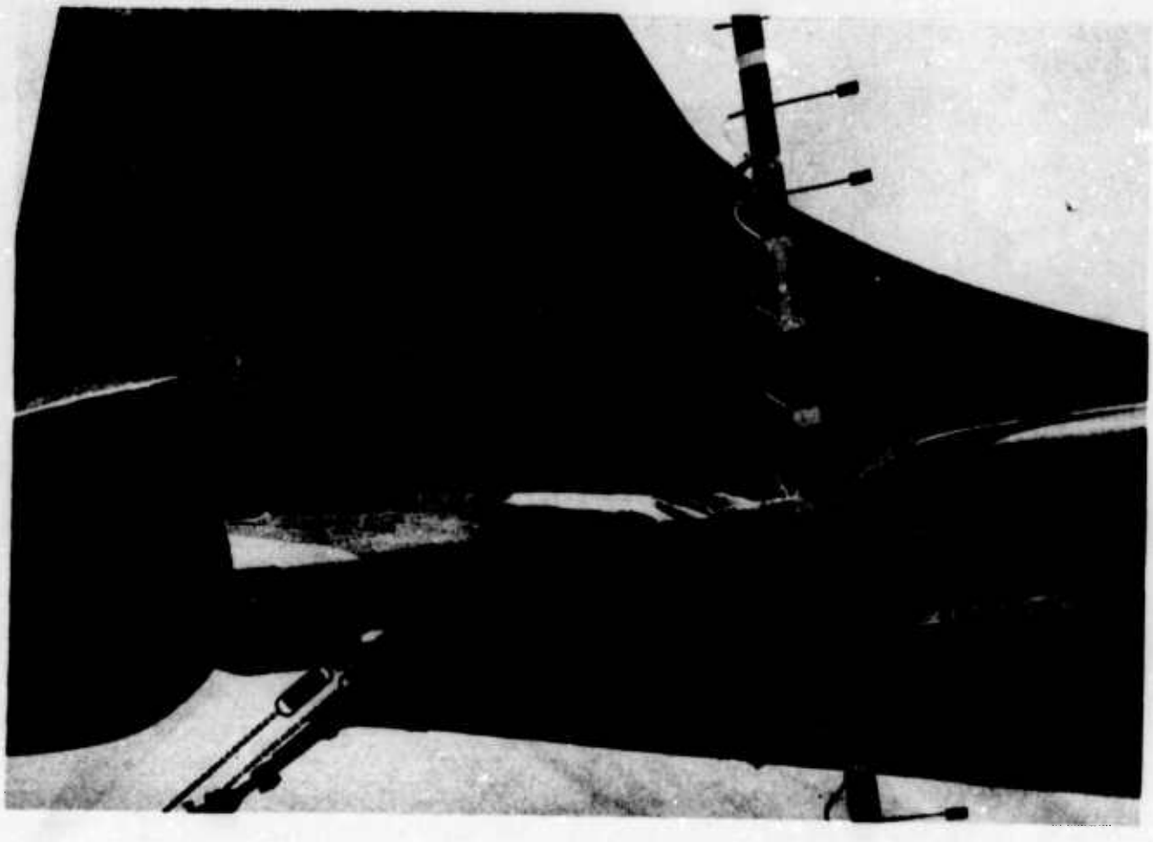

Figure 34. Wake Rake Used in Tailplane Studies.

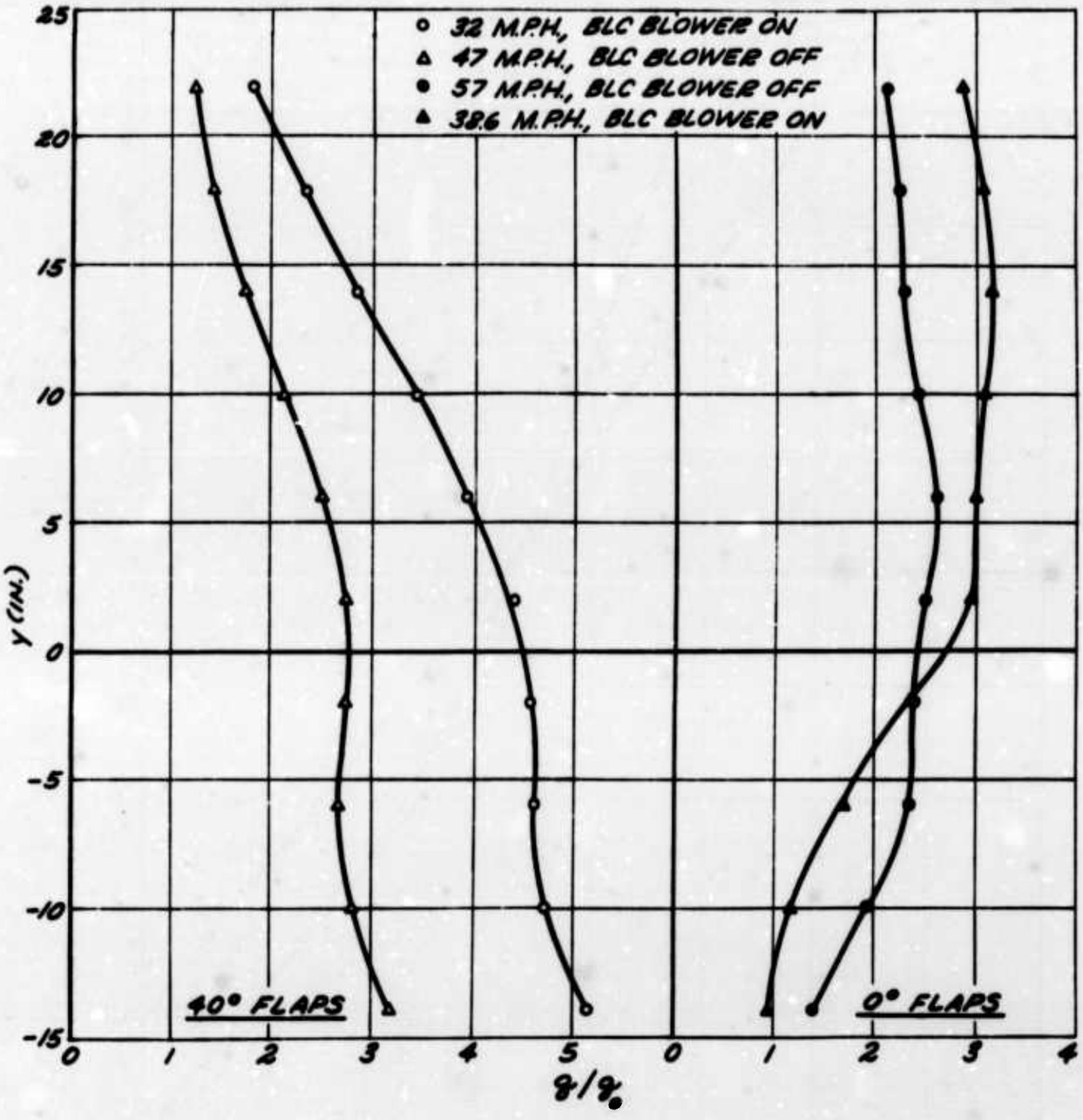

Figure 35. Results of Dynamic Head Survey at Tailplane, Level Flight Power.

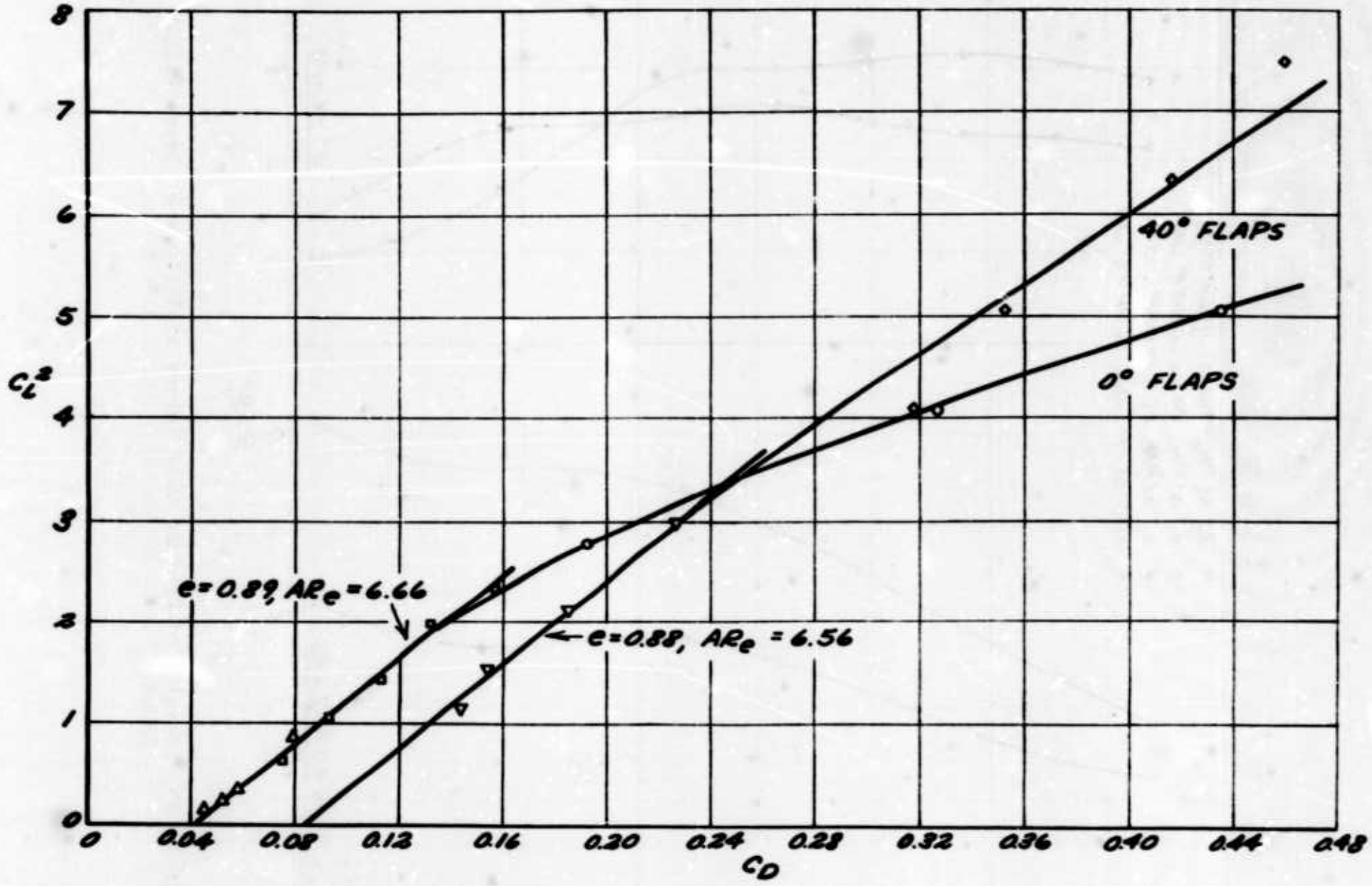

Figure 36. Linearized Drag Polar.

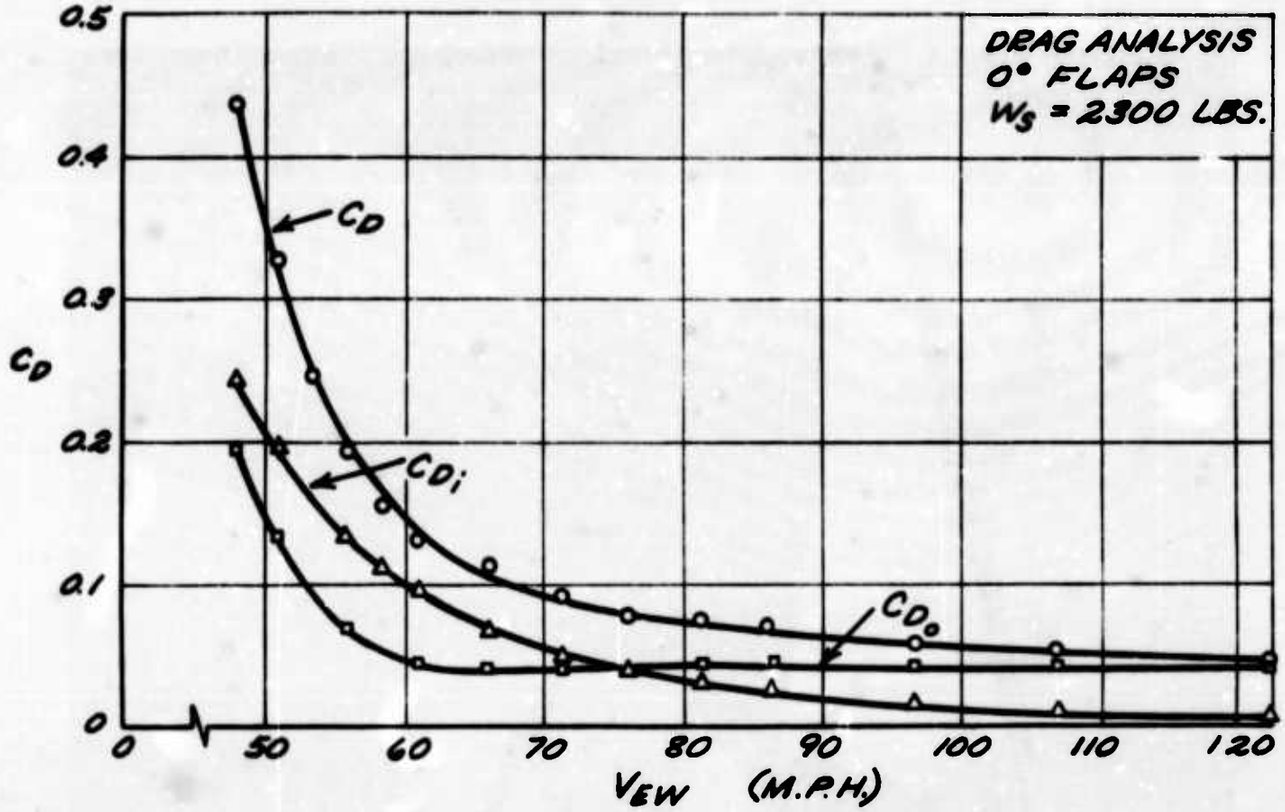

Figure 37. Drag Analysis - 0° Flaps.

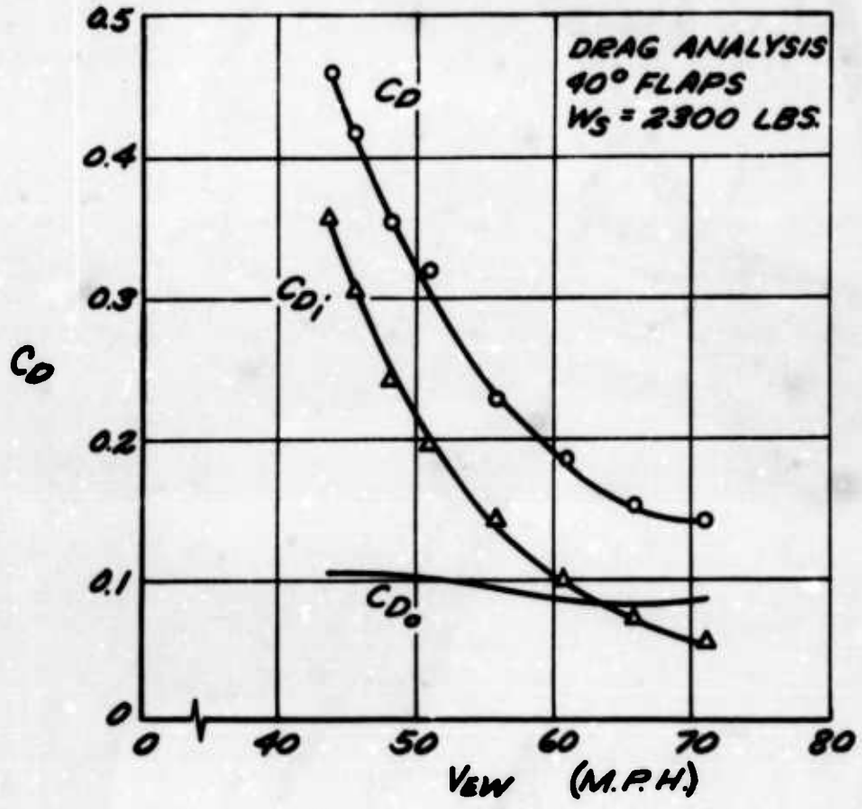

Figure 38. Drag Analysis - 40° Flaps.

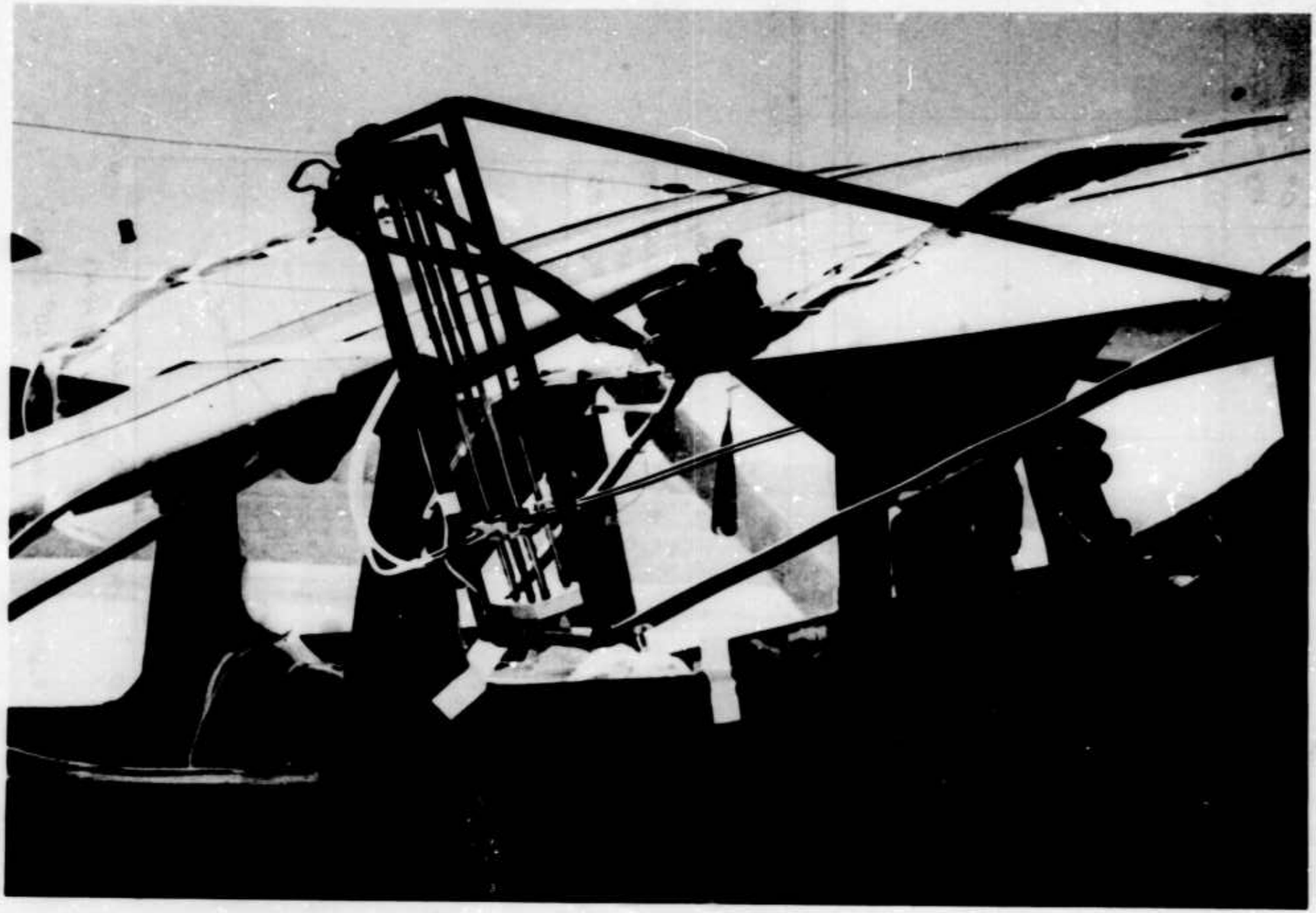

Figure 39. Wing Wake Traversing Rake.

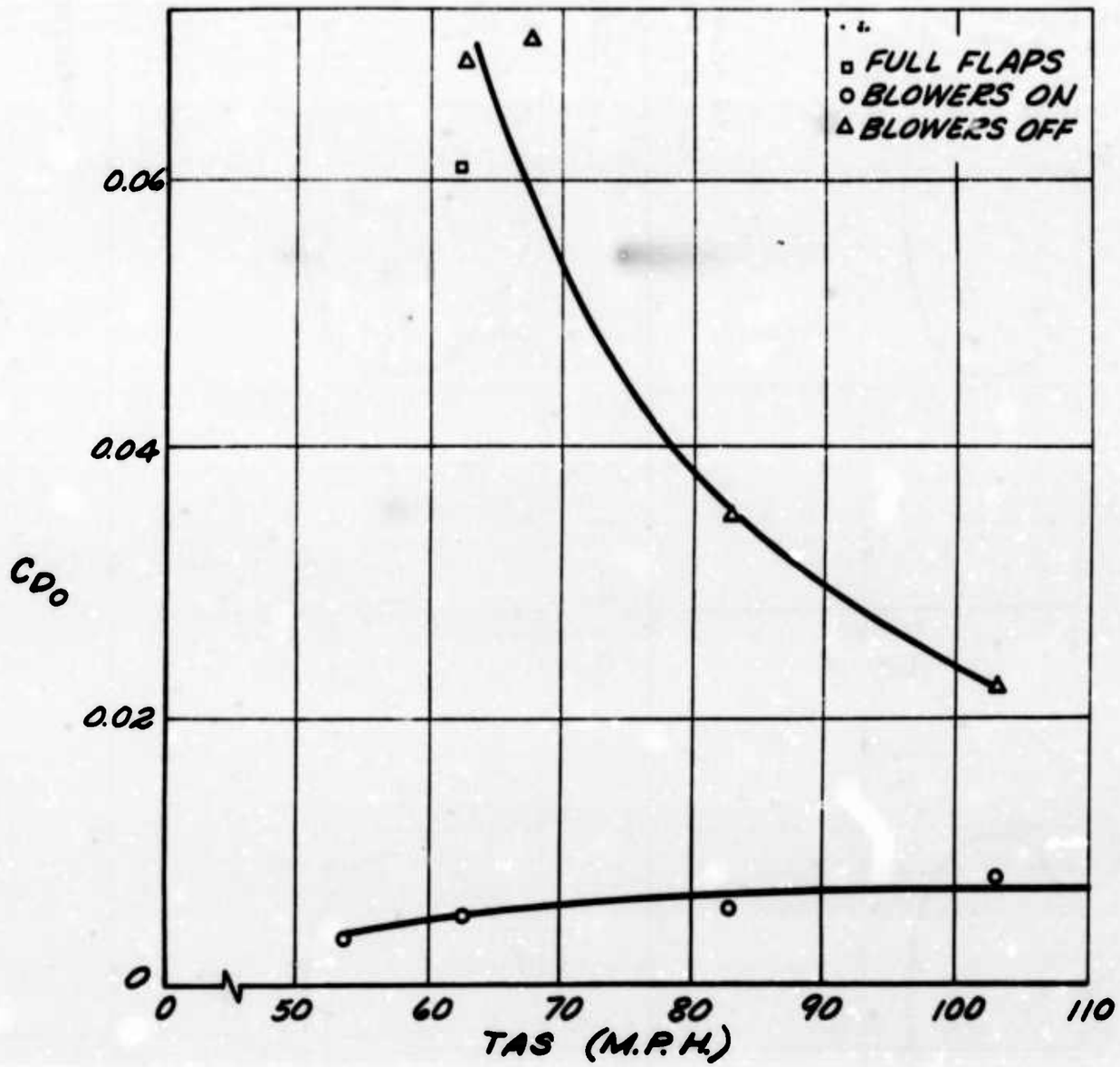

Figure 40. Wing Profile Drag.

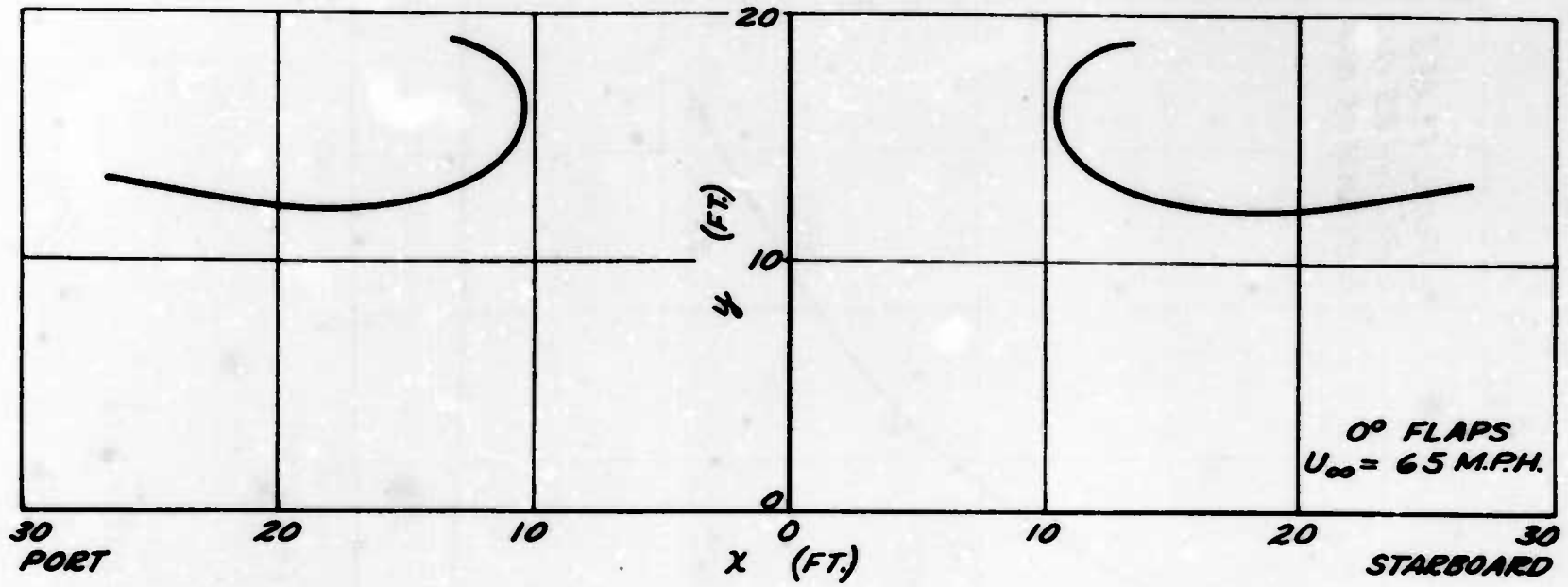

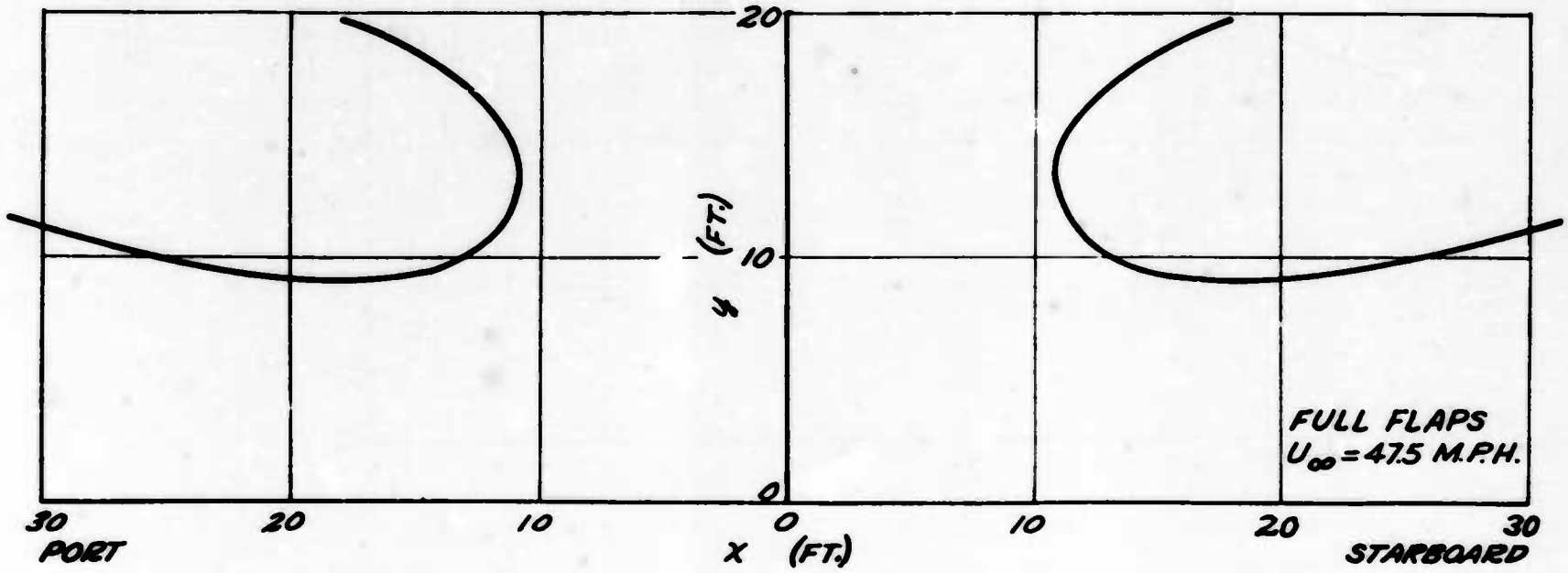

Figure 41. Path of Motion of Wing Vortices.

BIBLIOGRAPHY

1. Clark, D. G., "Flight Development of a High-Lift Research Aircraft Using Distributed Suction", Advisory Group for Aeronautical Research and Development Flight Mechanics Panel, Paris, France, June 1965.

2. Cornish, J. J., III, A Comparison of the Power Requirements of Distributed Suction and Jet Blowing to Increase Lift, Aerophysics Department, Mississippi State University, State College, Mississippi, May 1959.

3. Cornish, J. J., III, "Some Aerodynamic and Operational Problems of STOL Aircraft with Boundary Layer Control", Journal of Aircraft, March 1965.

4. Davidson, J. D., and Ferry, R. G., TL-19D Phase IV Performance, Air Force Flight Test Center Technical Report 57-14, Defense Documentation Center No. AD-124109, Washington, D. C., July 1957.

5. Fisher, J. W., et al, Flight Test Results on the Use of High-Lift Boundary Layer Control Applied to a Modified Liaison Airplane, Defense Documentation Center No. AD-92459, Washington, D. C., March 1956.

6. Head, M. R., Clark, D. G., and Wells, P. M., Flight Research on Suction for High-Lift, Progress Report, Cambridge University, England, 1964.

7. Ludweig, H., and Tillman, W., Investigation of the Wall-Shearing Stress in Turbulent Boundary Layers, Technical Memorandum 1285, National Advisory Committee for Aeronautics, (Translation), Washington, D. C., May 1950.

8. Pinkerton, Robert M., Calculated and Measured Pressure Distributions Over the Midspan Section of the N.A.C.A. 4412 Airfoil, Technical Report No. 563, National Advisory Committee for Aeronautics, Langley Memorial Aeronautical Laboratory, Langley Field, Virginia, 1936.

9. Roberts, Séan C., and Smith, Michael R., Flow Visualization Techniques Used in Full Scale Flight Tests, Research Report No. 49, Aerophysics Department, Mississippi State University, State College, Mississippi, April 1964.

10. Strier, J., Phase II Flight Tests of the TL-19C Aircraft, Air Force Technical Report No. AFFTC-54-9, Defense Documentation Center No. AD-33465, Washington, D. C., 1954.

11. Theodorsen, Theodor, Theory of Wing Sections of Arbitrary Shape, Technical Report No. 411, National Advisory Committee for Aeronautics, Langley Memorial Aeronautical Laboratory, Langley Field, Virginia, 1931.

APPENDIX I

DATA ON L-19

The Cessna Army L-19 (111972) equipped with the distributed suction boundary layer control system is powered by a Continental Motors 0-470-11 engine rated at 213 horsepower at 2,600 r.p.m. The modifications to the aircraft are a smooth upper-wing surface with flush rivets and an increased leading edge radius. The original single-slotted flaps were replaced by a sealed camber changing flap. The upper surface of the wing and flaps was perforated to accommodate the boundary layer control system. Hydraulically powered axial fans, driven by a pump mounted on an accessory pad on the engine, are mounted on each wing behind the strut, and the original strut has been replaced by a cylindrical pipe to improve the flow over the wing at high angles of attack. End plates are found at the outboard extremity of the flap and horizontal stabilizer. Dimensional data are as follows:

Wings:	Area	174 feet^2
	Span	36 feet
	Chord at Root	5.33 feet
	Chord at Tip	3.58 feet
	M. A. C.	4.87 feet
	Airfoil Section	NACA 2412
Flaps:	Area	21.2 feet^2
	Span	8.85 feet^2
	Chord	1.605 feet^2
	Max Deflection	42 degrees
Aileron:	Area	18.3 feet^2
	Span	8.85 feet
	Chord	1.03 feet
Horizontal Tail:	Area	19.23 feet^2
	Incidence	-4 degrees
	Airfoil	NACA 0006
Elevator:	Area	15.95 feet^2
	Span	10.55 feet
	Deflection	26 degrees up, 20 degrees down

APPENDIX II

LIFT COEFFICIENT DATA ON L-19

AIRCRAFT AIRSPEED AND LIFT COEFFICIENT DATA		
Aircraft Airspeed (m.p.h.)	Aircraft C_L	Local Section C_l
30.9	5.76	4.30
33.6	4.88	3.58
39.0	3.62	3.20
44.0	2.79	2.68
49.7	2.23	2.46
59.6	1.55	1.85
69.8	1.13	1.46
79.6	1.30	0.86

LIFT COEFFICIENT DATA AS A FUNCTION OF FLAP ANGLE			
Aircraft Airspeed (m.p.h.)	Aircraft C_L	Local Section C_l	Flap Angle (degrees)
39.5	3.52	2.84	0
39.5	3.52	2.78	15
39.5	3.52	2.73	25
39.5	3.52	3.06	40

Unclassified

Security Classification

DOCUMENT CONTROL DATA · R&D

(Security classification of title, body of abstract and indexing annotation must be entered when the overall report is classified)

1 ORIGINATING ACTIVITY *(Corporate author)*
Mississippi State University
Aerophysics Department
State College, Mississippi

2a REPORT SECURITY CLASSIFICATION
Unclassified

2b GROUP

3 REPORT TITLE
Flight Test Evaluation of a Distributed Suction High-Lift Boundary Layer Control System on a Modified L-19 Liaison Aircraft

4 DESCRIPTIVE NOTES *(Type of report and inclusive dates)*

5 AUTHOR(S) *(Last name, first name, initial)*
Roberts, Sean C.
Smith, Michael R.
Clark, David G.

6 REPORT DATE	7a TOTAL NO OF PAGES	7b NO OF REFS
June 1966	72	11

8a CONTRACT OR GRANT NO.
DA 44-177-AMC-265(T)

b PROJECT NO
Task 1P125901A14203

c

d

9a ORIGINATOR'S REPORT NUMBER(S)
USAAVLABS Technical Report 66-36

9b OTHER REPORT NO(S) *(Any other numbers that may be assigned this report)*
Aerophysics Research Report No. 66

10 AVAILABILITY/LIMITATION NOTICES
Distribution of this document is unlimited.

11 SUPPLEMENTARY NOTES

12 SPONSORING MILITARY ACTIVITY
U. S. Army Aviation Materiel Laboratories
Fort Eustis, Virginia

13 ABSTRACT

A distributed suction high-lift boundary layer control system fitted to a standard liaison L-19 aircraft increased the aircraft C_L max to 5.74 and decreased the take-off and landing distance over a 50-foot obstacle by 38 percent and 29 percent, respectively, with no increase in available power. The modified aircraft demonstrated acceptable stability, control, and handling characteristics in all flight phases, and the stalling characteristics were good, with no rolling tendency. Considerable structural modifications were necessary to obtain the above results. The small holes in the boundary layer control system operated quite successfully for a period of 5 years without clogging due to dust or rain.

DD FORM 1 JAN 64 1473

Unclassified

Security Classification

14. KEY WORDS	LINK A		LINK B		LINK C	
	ROLE	WT	ROLE	WT	ROLE	WT

INSTRUCTIONS

1. ORIGINATING ACTIVITY: Enter the name and address of the contractor, subcontractor, grantee, Department of Defense activity or other organization *(corporate author)* issuing the report.

2a. REPORT SECURITY CLASSIFICATION: Enter the overall security classification of the report. Indicate whether "Restricted Data" is included. Marking is to be in accordance with appropriate security regulations.

2b. GROUP: Automatic downgrading is specified in DoD Directive 5200.10 and Armed Forces Industrial Manual. Enter the group number. Also, when applicable, show that optional markings have been used for Group 3 and Group 4 as authorized.

3. REPORT TITLE: Enter the complete report title in all capital letters. Titles in all cases should be unclassified. If a meaningful title cannot be selected without classification, show title classification in all capitals in parenthesis immediately following the title.

4. DESCRIPTIVE NOTES: If appropriate, enter the type of report, e.g., interim, progress, summary, annual, or final. Give the inclusive dates when a specific reporting period is covered.

5. AUTHOR(S): Enter the name(s) of author(s) as shown on or in the report. Enter last name, first name, middle initial. If military, show rank and branch of service. The name of the principal author is an absolute minimum requirement.

6. REPORT DATE: Enter the date of the report as day, month, year; or month, year. If more than one date appears on the report, use date of publication.

7a. TOTAL NUMBER OF PAGES: The total page count should follow normal pagination procedures, i.e., enter the number of pages containing information.

7b. NUMBER OF REFERENCES: Enter the total number of references cited in the report.

8a. CONTRACT OR GRANT NUMBER: If appropriate, enter the applicable number of the contract or grant under which the report was written.

8b, 8c, & 8d. PROJECT NUMBER: Enter the appropriate military department identification, such as project number, subproject number, system numbers, task number, etc.

9a. ORIGINATOR'S REPORT NUMBER(S): Enter the official report number by which the document will be identified and controlled by the originating activity. This number must be unique to this report.

9b. OTHER REPORT NUMBER(S): If the report has been assigned any other report numbers *(either by the originator or by the sponsor)*, also enter this number(s).

10. AVAILABILITY/LIMITATION NOTICES: Enter any limitations on further dissemination of the report, other than those imposed by security classification, using standard statements such as:

(1) "Qualified requesters may obtain copies of this report from DDC."

(2) "Foreign announcement and dissemination of this report by DDC is not authorized."

(3) "U. S. Government agencies may obtain copies of this report directly from DDC. Other qualified DDC users shall request through

_____."

(4) "U. S. military agencies may obtain copies of this report directly from DDC. Other qualified users shall request through

_____."

(5) "All distribution of this report is controlled. Qualified DDC users shall request through

_____."

If the report has been furnished to the Office of Technical Services, Department of Commerce, for sale to the public, indicate this fact and enter the price, if known.

11. SUPPLEMENTARY NOTES: Use for additional explanatory notes.

12. SPONSORING MILITARY ACTIVITY: Enter the name of the departmental project office or laboratory sponsoring *(paying for)* the research and development. Include address.

13. ABSTRACT: Enter an abstract giving a brief and factual summary of the document indicative of the report, even though it may also appear elsewhere in the body of the technical report. If additional space is required, a continuation sheet shall be attached.

It is highly desirable that the abstract of classified reports be unclassified. Each paragraph of the abstract shall end with an indication of the military security classification of the information in the paragraph, represented as *(TS)*, *(S)*, *(C)*, *or (U)*.

There is no limitation on the length of the abstract. However, the suggested length is from 150 to 225 words.

14. KEY WORDS: Key words are technically meaningful terms or short phrases that characterize a report and may be used as index entries for cataloging the report. Key words must be selected so that no security classification is required. Idenfiers, such as equipment model designation, trade name, military project code name, geographic location, may be used as key words but will be followed by an indication of technical context. The assignment of links, rules, and weights is optional.

3791-66